Partly submerged crane suspended jacket

Koen Eijgenraam

June 2020

TU Delft

DELFT UNIVERSITY OF TECHNOLOGY
OFFSHORE & DREDGING ENGINEERING

Partly submerged crane suspended jacket

K.S. Eijgenraam
4319125

June 3, 2020

Graduation committee TU DELFT:
Dr.ir. S.A. Miedema
Dr. -Ing. S. Schreier
Dr. ir. M.B. Duinkerken

Graduation committee HEEREMA MARINE CONTRACTORS:
Ir. J. Bokhorst
Ir. P. Samudero

Department:
Dredging Engineering
Ship Hydromechanics
Transport Engineering Logistics

Position:
Lead Specialist Engineer
Specialist Engineer

TU Delft

MARINE CONTRACTORS

Abstract

This study is focused on the decommissioning of a jacket with a heavy lift vessel. During the transport the crane suspended jacket hanging in air can start swinging due to swell waves. This can result in undesired risks such as a collision between the jacket and the vessel. To prevent this undesired risks from occurring a solution must be sought. A possible contingency scenario to prevent this risks from occurring is to (partly) submerge the jacket. The aim of this study is to investigate in which way the jacket motion response changes if it would be in the water. A research methodology will be derived to investigate this. This will be done by investigating a jacket transport with the Thialf.

As a starting point, and for later comparison, the behaviour of the jacket in air, while it is free hanging from the cranes of the Thialf, will be investigated in a frequency domain solver Liftdyn. The resulting modes and response between the model and measurements indicate a good starting point. Thereafter the jacket will be lowered in to the water and the resulting forces will be determined.

The forces on the jacket will be determined using the linearised Morison equation. For the damping two approaches are investigated, i.e. the absolute velocity approach and the relative velocity approach. Subsequently different submerged depths are investigated and the effect of adding tugger winches is investigated.

The operability for the different scenarios is derived and compared. It is observed that by submerging the jacket the pitch mode is limiting the operability for wind waves. This mode can be damped by adding tugger winches. By submerging the jacket deeper the operability improves. For swell waves the operability is improved when the jacket is submerged.

It is concluded that submerging the jacket can be used as a contingency scenario for a swell train, but it is crucial to know the behaviour of the jacket. Because submerging it at the wrong depth could lead to large resonant responses. And by understanding the behaviour of the jacket tugger winches can be used to damp out a specific modes.

Preface

In front of you lies the document resulting from my master thesis project, in partial fulfillment to obtain the degree of Master of Science in Offshore and Dredging engineering at the Delft University of Technology. The project is a cooperation between the Delft University of Technology and Heerema Marine Contractors.

I would like to thank my supervisor from the university, Dr. -Ing. S. Schreier. I really appreciate the time you took to help me and guided me through the process.

Many thanks as well to Ir. J. Bokhorst and Ir. P. Samudero from Heerema for all their help during my research and showing me around in the world of a the marine contractors. Also thanks to all the other colleagues at Heeerema, I appreciate the interest and knowledge you have invested in my project.

Dr. ir. M.B. Duinkerken thank you for taking the time to take part of the committee. And last but not least thank you Dr.ir. S.A. Miedema for taking part in my committee as the chairman.

Contents

List of Figures

List of Tables

Acronyms

MME16	Motion Monitoring Equipment# 16
JONSWAP	Joint North Sea Wave Project
HMC	Heerema Marine Contractors
DP	Dynamic Positioning
KC	Keulegan Carpenter
Re	Reynolds Number
SPAR	Single Point Anchor Reservoir
TLP	Tension Leg Platform
CFD	Computational Fluid Dynamics
LAT	Lowest Astronomical Tide
DAF	Dynamic Amplification Factor
SDA	Significant Double Ampltiude
SMPM	Single Most Probable Maximum
PS	Port side
SB	Starboard
DNV	Det Norske Veritas
Aux	Auxiliary
CoB	Center of Buoyancy
CoG	Center of Gravity
SSCV	Semi-Submersible Crane Vessel
RAO	Response Amplitude Operator
OSPAR	Oslo-Paris convention

1

Introduction

In this chapter the general introduction to the subject, the company where this study is performed and decommissioning is presented. Also the relevance of the topic will be reasoned. Finally, a thesis outline is presented.

1.1. Platform decommissioning

Bottom founded structures

There is a wide variety of structures installed offshore, ranging from monopiles (with a diameter of a few meters) to Floating Production, Storage and Offloading units of almost 500 meters long. But most of the offshore structures that are build are fixed bottom founded platforms. They usually consist of a steel truss structure known as a jacket which is connected on the seabed with foundation piles. On top of the jacket is the actual production facility, the topside. The topside can consist of various modules. Usually there is a main deck, living quarters, a helideck, cranes, a power generation and production facilities. From this production facilities conductors and risers reach down to the oil or gas field.

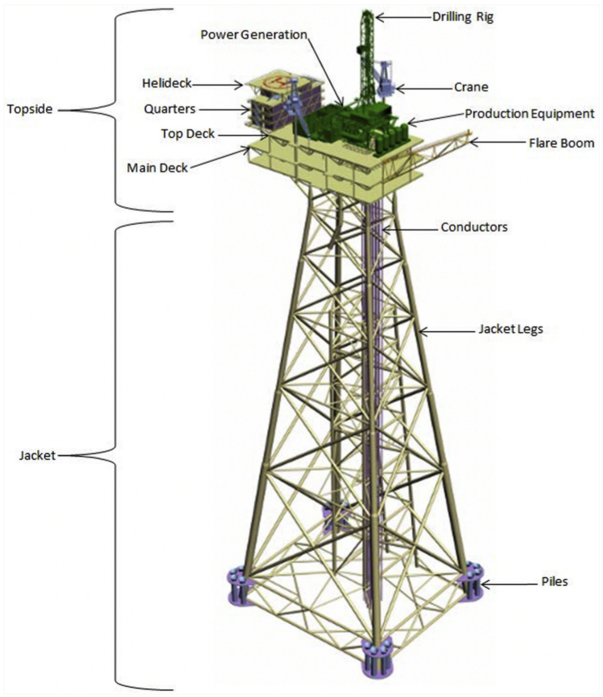

Figure 1.1: Bottom founded offshore structure components [4].

Decommissioning in the North Sea

From the 1970s platforms in the North Sea have been producing large amounts of oil and gas. Due to the discoveries of many oil and gas fields and the development of the oil price, the oil and gas industry have deployed many offshore structures in the North Sea since than. Since the area is relatively shallow water most of these structures are fixed steel jackets. After years of exploration and production many platforms in the North Sea are now entering a new phase of life, namely decommissioning. This has led to a relative new but big market for offshore contractors. They now have to remove the platforms which they installed years ago.

The OSPAR convention is the current legislative instrument regarding the mandatory decommissioning of platforms and protection of the environment at sea in the North-East Atlantic [7]. It is was signed in 1992 and it combines and updated the Oslo convention on dumping waste at sea and the Paris convention on land based sources of marine pollution, hence the name OS(lo)PAR(is).

According to the OSPAR legislation the following installations have to be removed. All installations have to be integrally removed apart from, fixed concrete structures (decks only) and 41 large steel platforms (> 10.000 t) (only partial removal). All steel platforms installed as from 1999 have to be removed totally. And the concrete platforms may only be installed if technical and safety considerations require their use and if removal at end of economic life is feasible. It is estimated by experts that around 600 installations will be decommissioned in the North Sea in the next 30 years [32].

Platform decommissioning phases

The decommissioning of such a bottom founded offshore platform typically consists of six phases. It can easily take several years of careful planning before the actual removal of a platform can begin. A lot of work needs to be done between the initial plan and the closure of the project. The different phases that are usually present are briefly described here [13].

Figure 1.2: Decommissioning phases

1. **Planning** - Develop, asses and select options. In this phase a global planning is made. Also the different possibilities of decommissioning are assessed and a preliminary option is selected.
2. **Permits** - Obtain approval and the necessary permits. Decommissioning activities are bound to national and international rules and regulations, to which the operator must comply.
3. **Stop production, P&A wells** - Stop the production and plug and abandon the wells. Also the facilities need to be cleaned so no oil or chemicals can spill in to the ocean.
4. **Detailed engineering and preparations** - In this phase the detailed engineering and preparations take place. A work plan needs to be drafted and approved and the specific parts prepared and/or made.
5. **Removal** - Removal of the structure, also known as decommissioning. This can be in parts or a one piece. The (parts of the) structures are lifted by a crane of a semi-submersible, mono hull or a jacket up. They are then transported to shore to start the next phase.
6. **Recycle** - Reuse and/or disposal of removed parts.

1.2. Decommissioning within Heerema

In this section the company profile will be given first. Thereafter the vessel and the jacket that are used in this study are introduced.

Heerema Marine Contractors

Heerema Marine Contractors, hereafter described as Heerema, is a world leading marine construction company for the oil, gas and the wind industry and is specialized in design, transportation, installation and removal of all types of fixed and floating offshore structures. Heerema owns and operates her own fleet including the world's largest semi-submersible crane vessel (SSCV), the Sleipnir, anchor handling tugs/supply vessels, cargo/launch barges and other equipment required for offshore activities e.g. pile driving hammers.

In this report the case study on the removal of a typical North Sea jacket with the Thialf is used. The Thialf and the North Sea jacket are briefly introduced here. The Thialf is a semi-submersible crane vessel operated and owned by Heerema. It is the second largest crane vessel in the world, after Heerema's other crane vessel the Sleipnir. The Thialf can perform a tandem lift of 14,200 ton. It is customized for the installation and decommissioning of jackets and topside, foundations, moorings, SPARs and TLP's. The overall length is 201.6m, the width is 88.4m and the draught can vary between 11.8-31.6m and it is equipped with a class III Dynamic Positioning system.

Figure 1.3: SSCV Thialf with the Jacket [28].

North Sea jacket

The platform was installed in the Norwegian sector of the North Sea. The details of this platform are given here. It was developed with a wellhead facility and a simple process plant. It was used to produce gas and gas condensate. It was remotely operated from another platform nearby. When the production was ceased the decommissioning contract was awarded to Heerema. Heerema removed the jacket, weighting approximately 6000 t and 150 m in height, with the Thialf in 2019. The jacket was lifted from the seabed and tilted horizontally (also known as downending). In Figure: 1.3 the jacket is almost fully the downended and out of the water. New in this operation for Heerema was that they transported the jacket having it suspended by the cranes only, instead of placing it on deck, a barge or restraining it to the SSCV. This method is called unrestrained crane suspended or 'free-hanging'. Since this type of operation was new, a motion sensor was placed on the jacket in order to log/monitor the motions during the transport.

1.3. Relevance research topic

In this section the relevance of decommissioning the a platform or more general, the whole decommissioning industry, is explained. It will be discussed from different angles, from an industrial, a social and a scientific point of view.

Industrial

From an industrial point of view it is the aim to decommission a platform as efficient, safe and cheap as possible. Understanding and being able to predict the behaviour of the jacket once it is in the water is a contributing step towards that aim. To begin with the safety aspect, if the motions get damped when the jacket is partly submerged this could be included as contingency scenario for undesired dynamic behaviour during transport. The efficiency can be increased if the behaviour of the jacket in the water is known since it could potentially widen the window in which the operation can be executed. Also the costs can be reduced by omitting the restraint since there is less offshore time needed and the restraint system does not have to be designed and manufactured.

If the results of this study are positive it creates the opportunity for further research. With the behaviour of the jacket in the water known the possibility of "wet transport" can be investigated. Transport in air is not always possible due to the increasing dimensions, weight and complexity of the jacket. By partly submerging the jacket these problems could potentially be solved:

- Change the dynamic behaviour due to having the jacket in water instead of air;
- Submerging the jacket reduces the hookload (due to buoyancy);
- By partly dragging the jacket through the water the height is less limiting.

Besides Heerema there are more companies looking in to the possibilities of wet transport. Saipem UK performed model tests at Marin to enhance its knowledge of the SSCV S-7000 and the jacket from Frigg QP platform during lifting and transporting it. They where interested in the sling loads, clearance and the global motions and accelerations [2]. The S-7000 decommissioned the jacket later in 2009.

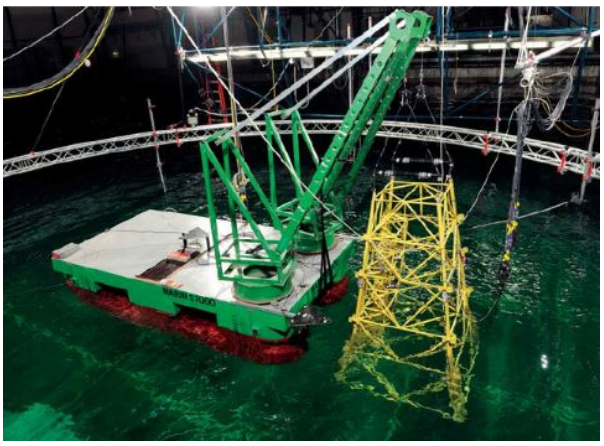

Figure 1.4: Marin model tests S-7000 with Frigg QP jacket [2].

Figure 1.5: Frigg QP jacket on wet transport [3].

Apart from the Frigg QP jacket also other projects have been executed. Saipem performed at least two other wet transports the last decade, the Ekofisk 2/4s jacket in 2014 and the Miller jacket in 2016 [34]. Other smaller scale projects have been carried out, like the Scaldis L6-B for example where they transported a tripod with the tips of the bucket slightly submerged.

The further research possibility for Heerema, the examples and the studies done relating this topic show that there is a larger interest in the effects of submerging jacket and possibly even wet transport it. This thesis provides a necessary step in that direction.

Societal

From a societal point of view the challenge is mainly in what to do with all the thousands of tons of old steel that is currently out in the North sea and in the other seas and oceans. Once a platform reaches the end of its lifetime there are three options, i.e. they will be scrapped, they will be relocated or they will be left in place. All three options will be explained in this section.

The first option, which is used for most of the offshore platforms, is that they will eventually be brought to shore by their owner to be scrapped. This is where offshore really meets the society. Recycling is the most environmentally-friendly solution. But recycling of a rig can be a heavy and a hazardous process. Workers, the environment and communities are exposed to a wide variety of risks such as toxic metal. There are two types of scrapping yards, the first one is on the beach and the second one is off the beach. In 2018 86% of the world end-of-life tonnage (not specifically oil & gas structures) where scrapped under rudimentary conditions on the beaches of South Asian countries according to Jenssen [15]. Since most beaching yards do not have the right infrastructure, procedures and equipment in place they can not fully contain and control the pollution, the safe handling and disposal of hazardous waste. You may have reservations about environmental friendliness in this case. But it can be done in a much more sustainable way, namely the second category, off the beach. The European Union made a list of around 45 facilities world wide that can recycle in a safe and sound way [40].

Figure 1.6: Workers dismantling ships in Alang, India [15]

Figure 1.7: Dismanteling yard AF Gruppe, Norway [9]

The second option for a offshore platform is to be relocated. The options here are to put (parts) of the platform on sale in the market, reuse in own company or return it to manufacturer for refurbishment. An example of a whole platform relocation is the Ophir platform of Vestigo. SPT Offshore lifted the entire platform for approximately 50 nautical miles where the platform was immediately reinstalled [27].

The third option is to leave the platform in the water. To just leave it in the water could cause potential dangers. The platforms could break down in an uncontrolled manner eventually causing pollution and other dangers. It could result in unknown obstacles for the shipping transport industry, which is highly undesired. A more viable option here is to clean the platform, decommission the topside and turn the jacket into a artificial reef. This method is called rigs-to-reef. The jacket is placed on the seabed and creates an artificial reef. This method is not possible for all jacket and in all locations. But for the cases where it is possible it can attract a rich diversity of marine life. This can enhance the commercial and recreational fishing and diving activities. For the environment and operator it can also be beneficial since it saves fuel emissions for the transport and the jacket does not have to be scraped [25].

Figure 1.8: Rig-to-reef [25].

For all the three options lifting the platform or the jacket with a vessel is needed. Therefore it is, also from a societal point of view, important to get a better understanding of the jacket motions while it is hanging from the cranes of a vessel. Because the more information known up front, the better the decision can be made of what to do with the platform. Hereby keeping in mind that decommissioning of a platform is still not always done in an ethical and sustainable way.

Scientific

A gap analysis will be performed in this literature study. The theory behind it is applicable for other cases too. The methodology can also be used on a mono-hull or on an other jacket. The insights gained here could also be taken into consideration for the upending process of a jacket during installation or the transportation of a monopile of a wind turbine. For the upending process of a jacket the free hanging stage is usually much shorter if the dynamics stay the same. For the long monopiles partly submerging them during transport could help for the same reasons that submerging a jacket could help, as described in the industrial relevance section. In this case it might become possible then to transport long monopiles with less height requirement on the cranes or to lift even longer monopiles with the current cranes.

1.4. Thesis outline

This thesis is structured as follows. First a general introduction will be given in the first chapter. A general introduction in to the decommissioning of a platform will be given and the company at which this research was conducted will be introduced. Also the relevance of the research will be treated. The problem statement is at the centre of the second chapter. The scope definition and the research question will be presented. Thereafter the theoretical framework is given in Chapter 3.

The model of the crane suspended jacket decommissioning with the jacket hanging in air will be investigated in Chapter4. The measured data during the campaign is compared to the model predictions (based on Heerema's current practice) of the free hanging jacket transport in air. It is the aim to determine how well the free hanging jacket motions are predicted by the model and it will later be used as comparison for the submerged jacket.

In Chapter 5 the jacket will be submerged by lowering the jacket in the model determined in the previous chapter. Since the jacket is now in the water the relevant forces and the impact on the resulting motions will be determined. Based on the outcome of the first model with the absolute velocity approach and the literature from section 3.5 a updated approach is investigated and implemented. The verification will be performed in Chapter 6.

The results of the models are given based on the operability in Chapter 7. For the different scenarios and methods the operabilities are compared. Finally, the conclusions and recommendations are presented in Chapter 8. The research question(s) are answered and recommendations are made.

2

Problem statement

In this chapter the problem statement will be described. Where the problem originates from, what the problem is that arises and what the different stakeholders have for objectives. In the scope it is defined what is going to be investigated and also what is not. From all of the above mentioned follows the research question.

2.1. Origin

In the summer of 2019 the Thialf removed and transported a jacket and a topside using the new 'free hanging' method for the first time. During these transportation HMC placed a motion sensor on the suspended load in order to log/monitor the motions during the transportation. A new potential contingency scenario was though of during the campaign. In case of undesired dynamic behaviour of the jacket it could be partly lowered in to the water to introduce added damping into the system. Since it is unclear if, and if so how, it would damp the behaviour of the jacket it was concluded that a detailed study into this scenario was needed before implementing or using it for a project.

2.2. Problem statement

There are approximately 600 platforms in the North Sea that are going to be decommissioned in the coming decades. This creates a relatively new and big market for the offshore contractors. They now have to remove the platforms that they once installed. Although it sounds similar there are significant differences between decommissioning and installing a platform. The platforms have been out in the seas for many years which could lead to degradation of the structure, there can be damage and the exact drawings are not always available. Furthermore the margins on the removal are much smaller than for installation. Since the value of the asset for the oil- or gas-company is much less then when it was being installed. Additionally the oil price dropped in the economical crisis last decade, which reduces the overall margins in the offshore industry.

Due to the large number of platforms and the differences described above there is a desire to decommission the platforms as efficient and cheap as possible without lowering the safety level of the operation.
In the past jacket and topsides were decommissioned by the piece-small method or reverse installation. In both methods separate modules or pieces are lifted off the platform onto the deck of the lifting vessel or a barge. The downside of putting it on a barge is that the workability is low since there are two moving vessels. Also it requires the use of a barge (which costs money). There are three disadvantages to putting it on deck. Firstly, there is only very limited space available on the deck. Secondly, it is also not possible to lift something with the two cranes and put it on deck. And thirdly, additional lift height is needed to be able to put it on the deck. After that the heavy lifting vessels went on to single lifts, where the entire topside or jacket is lifted in one piece and restraint to the vessel or restraint on a barge. Deck space on the vessel is limited so lifting the entire structure on the deck is usually not possible. Due to the low workability putting it on a barge is not an popular option. The restraints to the vessel are mainly applied with the objective of increasing the stability of the vessel. However, when the stability is considered to be sufficient, it is possible to save offshore time and cost by omitting the restraints. And therefore transport the jacket unrestrained or 'free-hanging'.

Unrestrained crane suspended transport is a relatively new way of working for Heerema. Although this method has advantages there are also additional criteria that must be considered compared to the restraint transportation. The jacket is now able to move relative to the vessel. Undesired dynamic behaviour of the jacket can induce new risks to the operation.The prescribed vessel motion limits can be exceeded, the motions and forces on the jacket can damage it, the sling dynamics change, the clearance between the jacket and the vessel can become insufficient and last but not least cranes (fatigue) damage could occur.

2.3. Objectives

Since there are three stakeholders involved here there are multiple objectives. First there is Heerema, secondly the Delft University of Technology and lastly the author of this report.

As one of the stakeholders Heerema wants to reduce the risks as described above and if possible increase the range of jackets that can be decommissioned in a single piece. But there is currently no clear methodology on how to model the behaviour of the jacket if it is partly in the water (during transport). It is desirable for them to have such a methodology. It will be used to gain insight in the effect of lowering a jacket partly in the water (during transport) on its hydrodynamic behaviour. This is of important for two reasons. Firstly, the submerging of the jacket could be a contingency scenario to suppress undesired dynamic behaviour of the jacket during transport in air. Secondly, it could be a solution for transporting jackets which could otherwise not be transported in one piece. Free hanging transport in air is not always possible since jacket are becoming larger, heavier, more complex. Furthermore, not all jackets can be down-ended. If so, the clearance between the crane tip and the waterline can be insufficient.

As the second stakeholder, Delft University of Technology, it is of interest to get a better understanding of the response of the system. Therefore the objective is to derive the methodology for the(hydro-)dynamic response for the multi body system consisting of the jacket, the vessel and the auxiliary equipment.

And the last stakeholder is the author of this report. Within this thesis the first part of Heerema's objective is going to be addressed by setting up a methodology to derive the (hydro-)dynamic response for the multi body system. And with that methodology determine whether or not submerging the jacket could work as a contingency scenario. And suggestions/recommendations will be made with respect to further research/methods and the approach. The last objective of the author is to obtain the degree of Master of Science in Offshore and Dredging engineering at the Delft University of Technology.

2.4. Scope definition

This study focuses on how decommissioning of a jacket is done. On the free hanging transport of a jacket with a SSCV. And within of this transport only a potential contingency scenario will be investigated. Where the vessel stopped sailing and the jacket is (partly) submerged. This is done to study what happens if a jacket is partly submerged and on how to submerge it. The submerging of the jacket is going to be investigated to gain a better understanding in the effects at play. How the system changes once the jacket is submerged will be investigated based on the resulting response and operability. The lift off (of the seabed) and set down(at the yard) are not thoroughly investigated, but are considered for the boundary conditions. They determine the minimum length between the spreaderbar and the jacket to be able to rotate it while lifting. Furthermore the resulting fatigue on the crane can be determined based on the motions and loads but it is left outside of the scope of this thesis. Within this study the Thialf with the North Sea jacket are used, but the method that is developed will also be applicable on other vessels and jackets.

The wind forces are neglected in this study. An in-house study from Heerema determined that the wind forces are very small compared to the other forces [10]. The vessel in waves is considered, but without forward speed, as also stated above. Forward speed is usually modelled as an equivalent current. Therefore current is not considered in the scope of this study. Also shielding of the jacket with the SSCV is not modelled, since waves are mostly coming from behind while sailing to the decommissioning yard during the North Sea jacket campaign. If shielding would be considered it is expected that smaller displacements, mainly for shorter wave period, will be experienced according to Slyozkin [33].

When the project is executed offshore a decision needs to be made on quite a short notice. Therefore it is desirable to be able to quickly identify, based on existing tools, if submerging the jacket could solve the potential problem.

2.5. Research question

From the problem statement and the associated objectives the following research question arises:

How does the response of a crane suspended jacket and the vessel change if the jacket is (partly) submerged in water compared to in air?

To answer this question the following sub-questions are formulated:

1. How does the free hanging jacket in air behave?
2. What are the relevant forces and how can they and the resulting motions be determined?
3. How should one submerge the jacket to reduce the motions as much as practically possible based on a case study of the North Sea jacket?

3

Theory

In this chapter the theoretical framework will be presented. The theories will be presented generally first, in the last section they will be linked to the problem of this thesis. The framework will be presented by first looking in to how waves are characterized. Then it will be investigated how the resulting wave forces can be determined on a structure and how these forces can be translated in the motion of the structure. After all the theory is presented it will be analysed how this theory is going to be used in this study and the reason why.

3.1. Waves

In this section the theory to characterize waves will be explained. The wind or a storm can generate waves at open water. Those waves are typically irregular. But they can be seen as a superposition of many regular harmonic wave components. This is called the superposition principle and is given in Figure: 3.1.

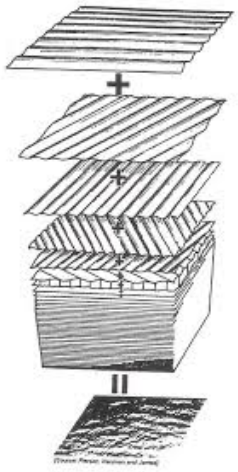

Figure 3.1: Principle of super position of waves. [16].

To analyse a complicated wave system, it is necessary to know all the components of the regular wave components. The wave components can be described by (airy) linear wave theory [16]. Each wave with its own height (H), length(λ), period (T) and direction. An example of such a regular wave is given in Fig: 3.2. The wave, at a certain location in space (x) and time (t), can be described by the wave elevation (ζ). The elevation depends on space, time, the wave number (k), the wave frequency (ω) and the wave amplitude (ζ_a). The wave amplitude describes the distance between the wave peak or trough with respect to the still water level (SWL).

$$\zeta = \zeta_a cos(kx - \omega t) \tag{3.1}$$

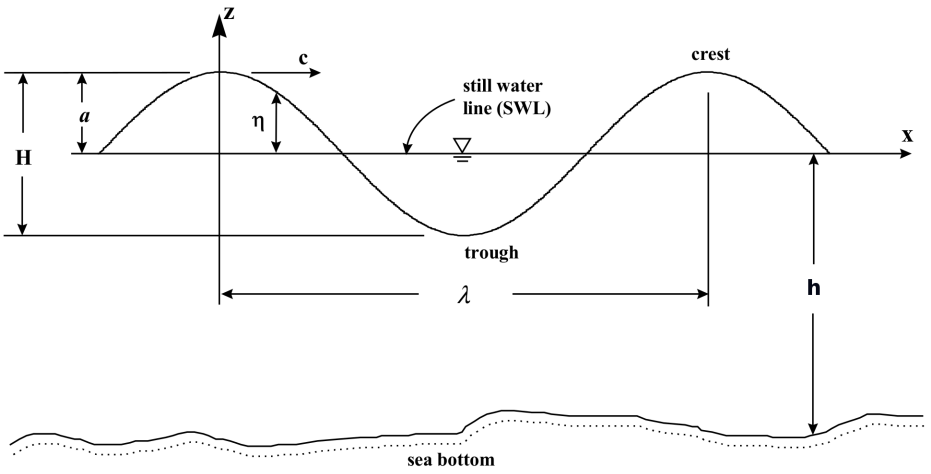

Figure 3.2: Regular wave [16].

The following characteristics are important here. And can be determined as followed:
The water depth h is the distance between the seabed (z=-h) and the still water level (z=0).
The wave height is measured vertically between the wave trough and wave crest.

$$H = 2\zeta_a \tag{3.2}$$

The dispersion relation describes the frequency dispersion, which means that waves of different wavelengths travel at different phase speeds. For deep water $tanh(kh) \approx 1$.

$$\omega^2 = gk \cdot tanh(kh) \tag{3.3}$$

The wavelength is the distance over which the wave's shape repeats. And can be calculated based on the wave period (T) for deep water:

$$\lambda = \frac{g}{2\pi} T^2 \approx 1.56 T^2 \tag{3.4}$$

The wave number defined as the number of radians per unit distance and can be calculated as:

$$k = \frac{2\pi}{\lambda} \tag{3.5}$$

The water is considered deep if the waves do not "feel" the seabed. This is the case if the depth is more than half the wave length, so $\frac{h}{\lambda} > 0.5$. And the water is considered shallow if the sea floor has a large influence on the characteristics of the waves. This is the case if h is less than $1/20$ of the wavelength, so: $\frac{h}{\lambda} < 0.05$.

The separate surface elevations ζ from Equation: 3.1 are used to calculate the water particle kinematics for waves [16]. The kinematics of a water particle is found from the velocity components in x- and z- directions. It creates a circular trajectory for deep water waves and a more oval path for shallow water waves, as shown in Figure: 3.3. The horizontal and vertical velocities are calculated based on the velocity potential in waves and the dispersion relation, Equation: 3.3, and are presented in the Equations: 3.6 and 3.7 respectively.

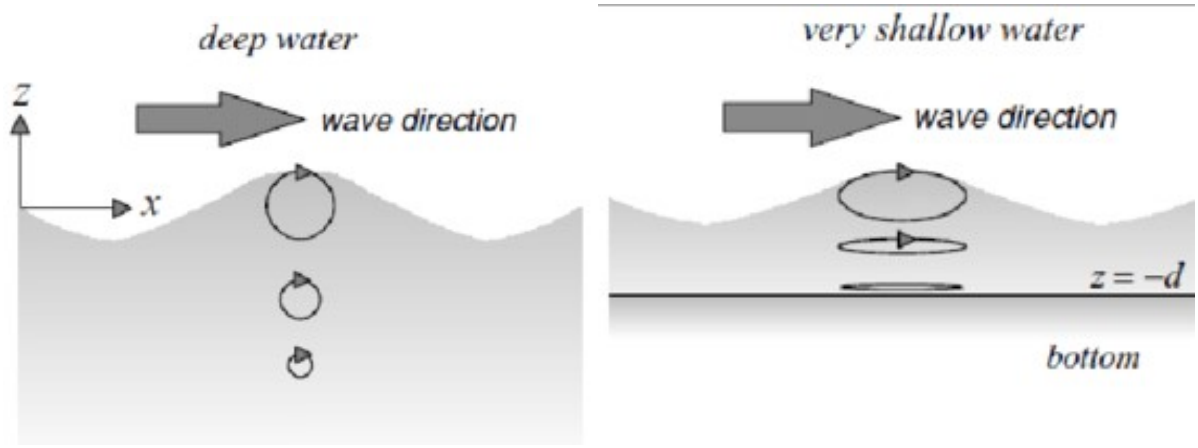

(a) Linear wave particle trajectories for deep water.

(b) Linear wave particle trajectories for shallow water.

Figure 3.3: Linear wave particle trajectories [12].

$$u = \frac{\partial \Phi_w}{\partial x} = \frac{dx}{dt} = \zeta_a \frac{kg}{\omega} \frac{coshk(h+z)}{coshkh} cos(kx - wt) \tag{3.6}$$

$$w = \frac{\partial \Phi_w}{\partial z} = \frac{dz}{dt} = \zeta_a \frac{kg}{\omega} \frac{sinhk(h+z)}{coshkh} sin(kx - wt) \tag{3.7}$$

In **deep water**, the wave particle velocities can be simplified and are given by:

$$u = \zeta_a \omega e^{kz} cos(kx - \omega t) \tag{3.8}$$

$$w = \zeta_a \omega e^{kz} sin(kx - \omega t) \tag{3.9}$$

The horizontal and vertical accelerations in deep water are obtained by differentiation of the velocity components with respect to time.

$$\dot{u} = +\zeta_a \omega^2 e^{kz} sin(kx - \omega t) \tag{3.10}$$

$$\dot{w} = -\zeta_a \omega^2 e^{kz} cos(kx - \omega t) \tag{3.11}$$

With the described theory above the individual wave components can be characterized. When describing an entire wave field the overall characteristics of the sea are usually more of interest. This is done with a wave spectrum as described below.

Wave spectrum

In 1969 an extensiv study was performed on young sea states in deep water with limited fetches. The research was named theJoint North Sea Wave Project (JONSWAP). The analysis of the data resulted in a JONSWAP wave spectrum, which is widely used for projects in the North sea. It is a modification of the Pierson-Moskowitz wave spectrum for fetch-limited(or coastal) wind generated seas. The following definition is advised in [16]:

$$S_\zeta(\omega) = \frac{320 H_{1/3}^2}{T_p^4} \cdot \omega^{-5} \cdot exp\left(\frac{-1950}{T_p^4} \cdot \omega^{-4}\right) \cdot \gamma^A \tag{3.12}$$

Where:

γ = 3.3 = Peakedness factor

$H_{1/3}$ = Significant wave height

T_p = Peak period

ω = Wave frequency

$A = exp\left(-\left(\frac{\frac{\omega}{\omega_p}-1}{\sigma\sqrt{2}}\right)^2\right)$

$\omega_p = \frac{2\pi}{T_p}$ = Wave peak frequency

σ = Spectral width parameter

3.2. Wave forces on structures

In this section the different theories and methods available to calculate the wave forces on a structure at sea are presented. Based on the wave theory described above different theories can be used. One can use the Morison equation, a diffraction analysis, Computational Fluid Dynamics (hereafter described as CFD) or perform (scale)model tests. Each theory or method has its own range of applicability. Dimensionless numbers or charts are often used to identify the flow patterns and which theory is thus best suited to use. The dimensionless numbers will be described first after which the different theories are explained in this section. The different theories are presented in this section. How these theories are going to be applied in this thesis is elaborated on in Section 3.5.

3.2.1. Dimensionless numbers

The Reynolds number (*Re*) is an important dimensionless quantity that is used to help predict the flow patterns for different fluid velocities. It indicates a flow regime from a smooth laminar flow, where viscous forces are dominant to a fully turbulent flow, which is dominated by inertial forces, see Figure: 3.4. The Reynolds number is calculated with Equation: 3.13. Another important dimensionless number is the Keulegan Carpenter number (KC), see Equation: 3.14, it is used for oscillating flows like waves. It assess the relative importance of drag force compared to inertial forces.

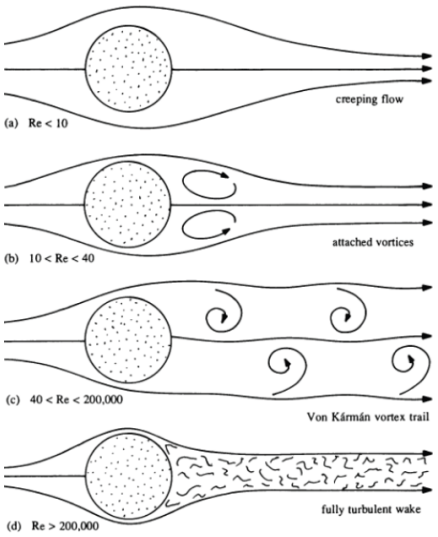

Figure 3.4: Flow around a cylinder for various Reynolds numbers [16].

For low values of KC (KC<3) the inertia force is dominant and drag can be neglected. For the next range until drag becomes significant (3<KC<15), drag can be linearised. And for the range 15<KC<45 the components are equally important. For high values of KC (KC>45) drag dominates and inertia can be neglected [5]. Sarpakaya carried out experiments and determined the Sarpkaya beta, β. It is another way of plotting but it is not something new since it can be rewritten as a function of the KC and Reynolds number [31].

$$Re = \frac{u_a D}{\nu} \tag{3.13}$$

$$KC = \frac{u_a T}{D} \tag{3.14}$$

$$\beta = \frac{D^2}{\nu T} = \frac{Re}{KC} \tag{3.15}$$

Where:

u_a= Flow velocity

D= Diameter of cylinder

ν= Kinematic viscosity

T= Wave period

Chakrabarti defined regions of application for three types of hydrodynamic forcing, inertial, drag and the forces resulting from wave diffraction. The different regimes are defined and plotted with the corresponding limits in Figure: 3.5, the Chakrabarti diagram [5]. The vertical axis is the equivalent to the KC number under the assumption of deep water. On the horizontal axis is a diffraction parameter, $\frac{\pi D}{\lambda}$, it is a measure for the size of the wave scattering from the structures. In the diagram are seven regions defined, region I through VI described different combinations of forces and the last region is above the deep water breaking wave curve, it that region the waves break.

For the first six regions, the higher the wave height becomes compared to the diameter the more important the drag forces are with respect to the inertia. The larger the structure becomes compared to the wave length the more important diffraction is. So to calculate the relevant forces on a structure the correct method must be chosen. For regions II a diffraction theory approach is eligible to calculate the hydrodynamic loads, which will be further on elaborated in Section 3.2.3.And for the regions III, V and VI a Morison equation approach is suitable, which will be further explained in Section 3.2.2. For region I the Morison equation or the diffraction theory approach can be used, since both theories can calculate the inertia correctly.

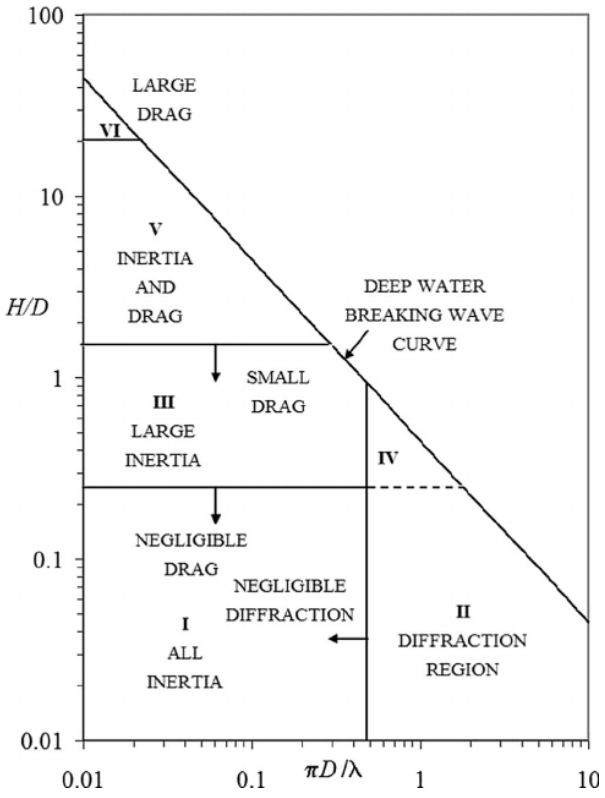

Figure 3.5: Different wave force regimes [5].

The dimensionless numbers and the Chakrabarti diagram will be used for the selection from the different theories that are presented in this section. This is done in section 3.5. But before the different theories are presented the marine growth is briefly explained. Since marine growth influences the outcome of all the different theories involved.

Marine growth

Within the offshore industry "marine growth" is the collective term for species that grow on or are attached to the structure below the waterline. One should think of mussels, barnacles, algae and seaweed for instance. This fouling of the surface has three influences. It changes the surface roughness, it changes the effective diameter of the structure and it adds mass to the system. The surface roughness has a direct impact on the drag and inertia coefficients as described in Section 3.2.2. Due to the fouling the vortex shedding from structure changes, the rougher the surface the more drag is experienced. Due to the layer of marine growth the effective diameter also changes. The layer thickest is highest near the surface and decreases with the water depth. The new diameter of the structure can be calculated by adding a layer to each side of the structure as $D_{eq} = D + 2 * t$. With the thickness as described by Norway Standards[24] and presented in Table 3.1. The mass of of the marine growth is to be added to the structural mass and added mass. The additional mass is calculated with the volume and the weight per volume of the marine growth from Table 3.1. It is given from the mudline to two meter above the Lowest Astronomical Tide (LAT). Note that the weight per volume for the in-air condition is equal to 9.0 $\frac{kN}{m^3}$ based on partial draining of the water from marine growth [10].

Table 3.1: Marine growth thickness and weight based on Elevation Level (EL) [24]. Note that the weight is weight per volume.

Elevation [m]	**Thickness** [mm]	**In-water weight** [$\frac{kN}{m^3}$]	**In-air weight** [$\frac{kN}{m^3}$]
From mudline, to EL(-)100	10	11.00	9.00
From EL(-) 100 to EL (-) 60	20		
From EL(-) 60 to EL (-) 40	30		
From EL(-) 40 to EL (-) 30	40	13.25	9.00
From EL(-) 30 to EL (-) 15	50		
From EL(-) 15 to LAT +2	60		
Above LAT +2	0	-	-

3.2.2. Morison equation

The Morison equation is derived to predict wave forces perpendicular to an exposed slender structure [22]. It superimposes the linear inertia force and an adaptation of the quadratic drag force per unit length for a (fixed) structure in an oscillatory flow. The assumption of this equation is that the submerged members on which the load is calculated do not affect the waves. This is valid for waves that are relatively large compared to the diameter of the member(s). According to Chakrabarti it is not valid to use Morison if $\frac{\pi D}{\lambda} > 0.5$. The DNV defined this limit stricter than Chakrabarti as $\frac{\lambda}{D} > 5$ [41]. If the diameter becomes larger compared to the wave length they start to affect the wave field, this is called diffraction. If that is the case the validity of the Morison equation can be compromised [39], since it is assumed that waves are not affected by the structure.

As stated above, the Morison equation is composed of a drag force and the inertial force. The drag force is related to the velocity and is created by viscous effects. The inertia force is related to the acceleration of water particles. The Morison equation depends on which effects are studied, whether the cylinder (or structure) is fixed, if there are waves and/or current and if the cylinder is oscillating in the water. First the original Morison equation is described after which the various possibilities for an oscillating cylinder are described. And at last the required coefficients for the drag and inertia are described. As stated above first the original Morison equation is given. The Morison force for a vertical fixed pile exposed to waves is given by Morison [22]:

$$F_{Morison} = F_{Inertia} + F_{Drag} = \underbrace{\frac{\pi}{4}\rho D^2 \frac{\partial u}{\partial t}}_{Froude-Krilov\ force} + \underbrace{\frac{\pi}{4}\rho D^2 C_a \frac{\partial u}{\partial t}}_{Added\ mass\ force} + \underbrace{\frac{\rho}{2} C_D D|u(t)|u(t)}_{Drag\ force} \tag{3.16}$$

Which can be simplified by combining the Froude-Krilov force and the added mass:

$$F_M = \frac{\pi}{4}\rho D^2 C_m \dot{u} + \frac{\rho}{2} C_D D|u(t)|u(t) \tag{3.17}$$

Where:

C_a= Added mass coefficient

C_m= Inertia coefficient, $C_m = 1 + Ca$

C_D= Drag coefficient

ρ = Water density

u = Fluid velocity

$\frac{\partial u}{\partial t} = \dot{u}$= Fluid acceleration

Oscillating cylinder in still water

The Morison equation was derived for a fixed cylinder in waves. If a cylinder is oscillating in still water the hydrodynamic forces related to the inertia are different. The Froude-Krilov will be absent in this case since the water is standing still so the ambient pressure gradient is zero. The inertia force will be associated to C_a and the Froude Krilov part from Equation: 3.16 is zero. The resulting Morison force will be depended on the body velocity and acceleration and acts in opposite direction of the body movement [31].

$$F_{M_{Still}} = -\frac{\pi}{4}\rho D^2 C_a \ddot{x} - \frac{\rho}{2} C_D D |\dot{x}| \dot{x} \tag{3.18}$$

Where:

$\dot{x} = \frac{\partial x}{\partial t}$ = Body velocity

$\ddot{x} = \frac{\partial^2 x}{\partial^2 t}$ = Body acceleration

Oscillating cylinder in waves

If the cylinder is moving in waves the total hydrodynamic forcing needs to be derived. This depends on the velocity and acceleration of the wave particle and the cylinder. For the inertia this can be done by combining the inertia parts of Equation: 3.16 and 3.18. For the drag related part this is different. Due to the quadratic term in the drag force a segregated treatment of the cylinder motion drag and the wave drag would lead to different forces, since :

$$u^2 + \dot{x}^2 < (u + \dot{x})^2 \tag{3.19}$$

Since the inertia is not quadratic it can be determined according to Equation 3.20 for each of the coming approaches. For the damping various approaches are proposed in the literature and will be discussed after the inertia.

$$F_{M_{Inertia}} = \rho V C_m \dot{u} - \rho V C_a \ddot{x} \tag{3.20}$$

The two approaches for the damping will be discussed below. First the relative velocity approach and then the absolute velocity approach. The first, and an apparent, approach is the relative velocity approach. It considers the relative velocity between the cylinder and the wave as [31]:

$$F_{M_{Rel}} = \frac{\rho}{2} C_D D |u - \dot{x}| (u - \dot{x}) \tag{3.21}$$

Notice here that due to the quadratic nature of the drag force it is not possible to split the (unknown) cylinder velocity from the wave velocity when computing the drag force. Thus it is not possible to calculate the time-dependent force component from the wave velocity independent of the dynamic response of the cylinder.

Since the superimposed jacket velocity, $\dot{x}$, is unknown, the solution must be obtained by iteration, for which special algorithms are proposed, like Van Wingerden and Stettner did for the floating installations of a jacket and a monopile [43],[36]. A step-by-step solution of the differential equation in the time domain is needed. Additionally a loop within each step must be performed to successfully approximate the resulting cylinder velocity [16]. That makes this approach a relatively time-consuming computation in time domain. An implementation of the relative velocity approach in frequency domain is not found during the literature study.

As the second approach the absolute velocity approach is considered. A strict interpolation of the the superposition principle is applied to the velocities. The forces resulting from the combined motions are treated as if they are fully independent of each other proposed by e.g. Laya and Sunder [17].

$$F_{M_{Abs}} = \frac{\rho}{2} C_D D |u| u - \frac{\rho}{2} C'_D D |\dot{x}| \dot{x} \tag{3.22}$$

This approach 'neglects' the cross term which one would get when writing out the quadratic velocity term from Equation: 3.21 ($-2u\dot{x}$). Usually the motions of the cylinder are considerably less than those of the surround water and therefore the largest contribution to the drag comes from the wave term. The advantage of this approach is now that the damping due to the velocity of the cylinder and the wave can be calculated separately. The wave related part can be isolated and moved to the right hand side of the equation of motion.

In a test with an oscillating horizontal cylinder in a uniform current, Moe and Verley [21] measured the forces on the cylinder. With a Cd and Cd' value. And they concluded that the relative velocity for the Morison equation is quite unconservative and over predicts damping in the system. Sarpkaya [31], on the other hand, recommended the use of relative velocity was better. As Cd' showed unrealistically high values.

Applicability of relative velocity formulation

When applying the Morison equation to a structure with waves and a constant current, the relative velocity approach is valid according to the DNV [41] if:

$$\frac{r}{D} > 1 \tag{3.23}$$

Where r is the member displacement amplitude and D the diameter of the member. When $\frac{r}{D} < 1$ the validity depends on the following parameter: $V_R = \frac{vT_n}{D}$ as follows:

$20 > V_R$ Relative velocity recommended.

$10 \leq V_R < 20$ Relative velocity may lead to an over-estimation of damping if the displacement is less than the member diameter.

$V_R < 10$ It is recommended to discard the velocity of the structure when the displacement is less than one diameter, and use the absolute velocity approach.

Where:

$v = v_c + \frac{\pi H_s}{T_z}$ = Approximate velocity

v_c= Current velocity

T_n= Period of structural oscillations

H_s= Significant wave height

T_z = zero crossing-up period

Inertia- and drag coefficients

The Morison equation,as seen in Equation: 3.16, depends on hydrodynamic coefficients which must be tuned for each specific case. The determination of these coefficients is based on measurements at full scale, model scale or CFD. A lot of research has been performed on these coefficients for various shapes under various flow conditions. Due to these experiments the behaviour of these coefficients is well captured for varying non dimensional numbers, like the KC and Reynolds number described in Section 3.2.1 or the surface roughness, ϵ (due to marine growth for example). Classification societies have determined standarized calculations to determine the inertia and drag coefficients. Depending on the design code or researcher different approaches are used.

Sarpkaya was one of the first researcher that described the dependency of the drag and inertia coefficient on the KC, Re and β. The results of the laboratory experiments using an U-tube are presented in Figure: 3.6.

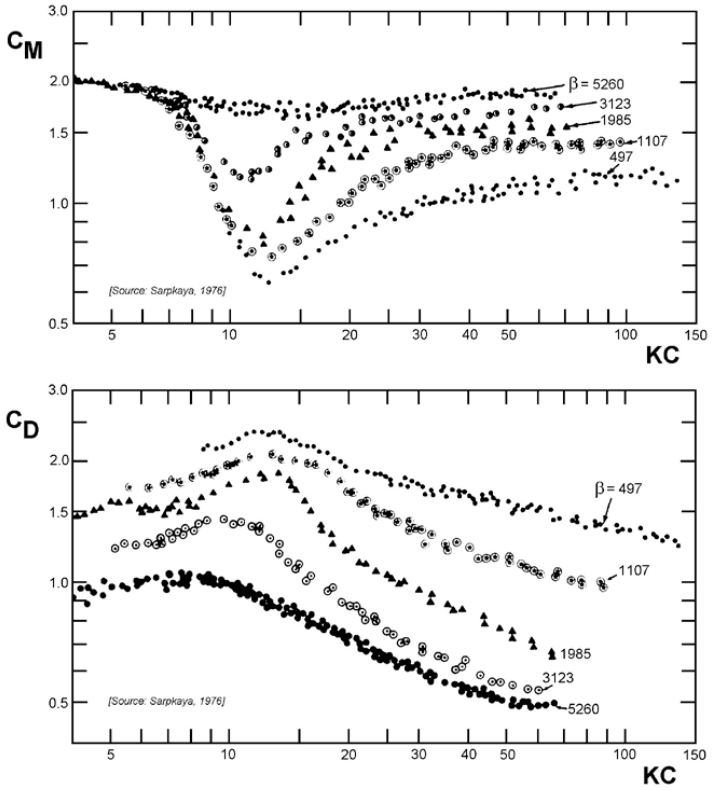

Figure 3.6: Inertia- and drag coefficients based on Sarpkaya [31].

The DNV and the API code are the most widely accepted and used codes in the industry for this. The API is the simplest approach of the two. It makes a difference for smooth or rough members, but does not consider the Reynolds number or the amount of roughness. The DNV code does include this effect. The values that DNV suggests are given in Figure: 3.7

Table 3.2: Inertia- and drag coefficients based on the API [29].

	C_D	C_M
Smooth	0.65	1.6
Rough	1.02	1.2

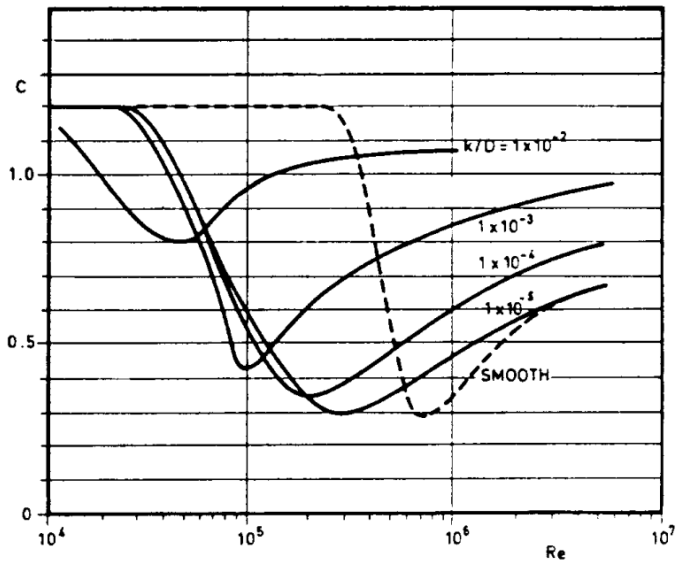

Figure 3.7: Drag coefficients based on DNV [41].

The Morison equation is now described for various flows. Also different ways to determine the corresponding drag and inertia coefficients are presented. An overview of the other theories is given below.

3.2.3. Other theories

Apart from the Morison equation there are other ways to calculate the wave forcing on a structure. Diffraction theory, CFD, Model tests. CFD and model tests are boths option which can perform tests on a very high level of detail. The downside of this is that they require very extensive preparation and are very time consuming. Therefore they are not considered in further detail in this study. Concerning the diffraction theory is, this will be considered in more detail. How this theory is going to be used in this thesis will be elaborated on in Section 3.5.

The diffraction theory is based on potential theory. A brief overview of the diffraction theory is given here. A more detailed explanation is given in Appendix A. It is assumed here that a rigid body is moving in an ideal fluid with harmonic waves. With potential theory the hydrodynamic loads are evaluated. The potential, $\Phi(x, y, z, t)$ is based on the superposition of:

- The undisturbed waves potential (Φ_w), this is the wave field as if the vessel is not there;
- The diffraction potential (Φ_d), these are the waves that reflect from the vessel;
- The radiated waves potential (Φ_r), which are the waves that radiate from the vessel due to the motions of the vessel. The waves that radiate are dissipating energy from the ship. This can also be referred to as potential damping.

3.3. Multi-body dynamics

In this section the dynamics required to determine the response of a body are described. With the different theories known to determine the wave forcing now the way to calculate the resulting motions is determined. The problem in this study consists of two main bodies, the Thialf and the jacket and some auxiliary equipment (spreaderbars and hooks). The main bodies are both affected by the waves and the water and they influence each other. Theories to calculate the wave forces are described in the section above. In this section the multi-body dynamics that are needed to understand how the bodies are influenced are described. Both bodies can move relative to each other but are connected, and thus influenced, by the crane cables, spreaderbars and hooks. In general each body can move in 6 degrees of freedom, three translations and three rotations. The convention with respect to the axes and the corresponding names and descriptions are given in Figure: 3.8. To calculate the motion or rotation of each degree of freedom equations of motion are needed. These equations can be solved in time domain or frequency domain, which will be elaborated on in the next section.

DOF	Name	Symbol	Unit	Description
1	Surge	x	[m]	Motion in x
2	Sway	y	[m]	Motion in y
3	Heave	z	[m]	Motion in z
4	Roll	ϕ	[rad]	Rotation around x-axis
5	Pitch	θ	[rad]	Rotation around y-axis
6	Yaw	ψ	[rad]	Rotation around z-axis

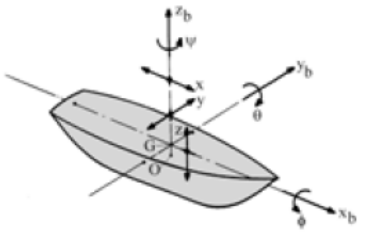

Figure 3.8: The Degrees of Free of a ship [16].

Time domain vs. Frequency domain

The equations of motion can be solved in a Time domain or Frequency domain approach. Either method has its advantages and its disadvantages, which will be elaborated on in this section.
In the time domain the equation of motion is solved every time step δt. This has the large advantage that in principle this method can solve any dynamics problem one can think off. The result is a simulation of the behaviour as we experience it in the real world. Since it solves the calculations at each time step the analysis itself is (very) time consuming and multiple simulation are required to obtain statistical reliable results. The **time domain** method is mainly applied for **non-linear** processes, with non linear differential equations. Such as, but not limited to, transient events like ballasting of a vessel, impact loads and mooring analyses.

The **frequency domain** approach can be used if it is governed by **linear** differential equations. So steady state harmonics where forces are linearly depending on the motion, velocity and acceleration. The advantages of the frequency domain approach is that it is very quick (time efficient) and easy to interpret the results. Due to the linearity the superposition principle can be applied. It states that the response caused by two or more stimuli is the sum of the responses that would have been caused by each one individually. This means that all different contributions that influence a multi-body system can be determined separately and then be added together to solve the whole systems response. The main disadvantage of this approach is that all non-linear aspects must be linearised first before they can be implemented. Like the quadratic Morison damping term, which will be further elaborated on in Section 3.5.

Due to all the disadvantages of the time domain approach and the advantages of the frequency domain approach and given the scope that a quick solver is desired and a frequency domain model is already available (for the jacket in air), the frequency domain approach is the preferred method.

In the frequency domain the response of a body will be with the same frequency as the excitation but usually with a phase angle between them. With the body motions **x** assumed as [16]:

$$\mathbf{x} = x_a e^{i\omega t} \tag{3.24}$$

The equation of motion for a system is given in Equation: 3.25. It is assumed that the system can be described by a set of mass-spring-damper system. Where in each body **M** is the mass matrix, **A** is the added mass matrix, **B** is the damping matrix, **C** the spring matrix and **F** the forcing vector [35]. The content of the matrices will be determined later.

$$(\mathbf{M}+\mathbf{A})\ddot{x}+\mathbf{B}\dot{x}+\mathbf{C}x=\mathbf{F} \tag{3.25}$$

Since the wave forcing factor is assumed harmonic it can also be written as [23]:

$$\mathbf{F}=Re(\mathbf{F}_a e^{i\omega t}) \tag{3.26}$$

With the complex amplitude,F_a depending on the wave amplitude, ζ_a and the complex wave transfer function $\mathbf{H}_{fz}$, which depends on the the wave frequency, the angle of which the waves are coming from and the outer shape of the body. And can be written as [23]:

$$\mathbf{F}_a=\mathbf{H}_{fz}\zeta_a \tag{3.27}$$

When substituting the motions vector as well as the new wave formulation it yields:

$$(-\omega^2(\mathbf{M}+\mathbf{A})+i\omega\mathbf{B}+\mathbf{C})x_a=\mathbf{S}\,x_a=\mathbf{H}_{fz}\zeta_a \tag{3.28}$$

The complex transfer function, also known as the Response Amplitude Operator(RAO) is based on this and given as [16]:

$$RAO(\omega)=\frac{\mathbf{x}_a}{\mathbf{H}_{fz}\zeta_a}=\mathbf{S}^{-1}\mathbf{H}_{fz} \tag{3.29}$$

From this the amplitude can be determined and the phase angle:

$$RAO_{amplitude}=\frac{x_a}{\zeta_a}=abs(RAO) \tag{3.30}$$

$$RAO_{phase}=\epsilon_x=angle(RAO) \tag{3.31}$$

Mode shapes and Natural frequencies

Mode shapes and their natural frequencies (also called eigenfrequencies) give a lot of insight in the behaviour of the model. They visualise what motions of the model are most important in different frequency regions. The natural frequency is a frequency at which a low amount of energy is required to oscillate the model. When a body is excited at those frequencies it can lead to the severe motions, much larger than the wave amplitude that triggered the motion. At every oscillation with a new excitation the amplitude of the motion increases, this is called resonance. The mode shapes and natural periods of the system are obtained by solving the following eigenvalue problem [16].

$$det(-\omega^2(\mathbf{M}+\mathbf{A})+\mathbf{C})x)=0 \tag{3.32}$$

3.4. Operability

In this section the operability will be explained based on the significant response, a wave spectrum and a set of limiting criteria. With that the operability curve can be derived. The operability curve gives, for each wave period, limit and response, a maximum allowable wave height before the limit is exceeded. They are presented in the $H_s - T_p$ curve and give the allowable sea states. First the significant response will be determined. Then the limiting criteria will be described. And lastly it is explained how the operability is determined.

Significant response

To determine the significant response the RAO of the response of interest is needed and a wave spectrum. In this study the JONSWAP spectrum is used. The wave spectrum is described in Section 3.1. From this the spectral response is determined which is used to calculate the significant double amplitude (SDA) [16].

$$S(\omega)_{motion} = |RAO(\omega)|^2 \cdot S(\omega)_{JONSWAP} \tag{3.33}$$

From the spectral response the zeroth spectral moment, m_0. This is also the area under the curve of the spectral response.

$$m_0(\omega) = \int_0^\infty S(\omega)_{motion}(\omega) \cdot d\omega \tag{3.34}$$

From the zeroth moment the significant double amplitude(SDA) can be determined [16]. Note that this is the double significant amplitude, provided that the wave spectrum is defined on the significant wave height, H_s, (which is double the significant wave amplitude).

$$SDA(\omega) = 4 \cdot \sqrt{m_0(\omega)} \tag{3.35}$$

With this SDA the Single Most Probable Maximum (SMPM) is determined. In this study the 3 hour SMPM is used, as suggested by DNV [42], in that period approximately a 1000 waves pass. For more details on the statistical derivation of the SMPM it is advised to consult Journee & Massee [16]or Holthuijsen [12] for example. The 3 hour SMPM single amplitude is determined as:

$$SMPM_{3hour}(\omega) = \frac{1}{2} \cdot \sqrt{\frac{1}{2} ln(1000)} \cdot SDA(\omega) \approx \frac{1.86}{2} \cdot SDA(\omega) \tag{3.36}$$

The SMPM for each of the responses will be used to determine the operability. But to determine the operability the operational limiting criteria are needed. And they will be explained next.

Operational limiting criteria

To determine the operability the operational limits are defined. This is done to protect the safety of the operation. Some limits are hard limits, like the clearance between the load and the vessel, others are derived based on experience by experts or the manufacturer. They are listed below:

1. Crane side-lead and off-lead
   The capacity of the cranes for side-lead and off-lead are an operational limiting criteria. Side-lead is defined as relative angle between the crane tip and the load perpendicular to the vessel. And off-lead as the angle between the crane tip and the load in line with the vessels surge direction. They are visualised in Figure:3.9.

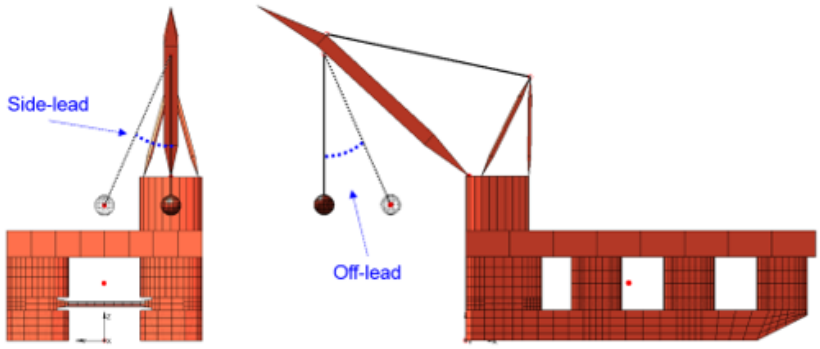

Figure 3.9: Crane side-lead and off-lead [30].

2. Clearance between the load and vessel
   A clearance between the load and the vessel must be preserved at all time. The minimal distance between the jacket and the Thialf during the transport is 8.4m, between the boom of the crane and the pile sleeves[28]. Therefore the limit is set to 6 meter to have some redundancy.

3. Hookload fluctuations
   The hookload fluctuations are described according to the Dynamic Amplification Factor(DAF). It is defined as described in Eq: 3.37. This is typically 1.1-1.3 during lifting operations in air and higher once submerged [1]. But it must stay below 2 to assure that there is no slack in the slings, which could lead to high snap loads. A limit of 1.3 in air and 1.9 in water is chosen for this study. When rewriting Eq: 3.37 it can be shown that this means that the $F_{dynamic} = 0.9 \cdot F_{static}$ maximal.

$$DAF = \frac{F_{total}}{F_{static}} = \frac{F_{dynamic} + F_{static}}{F_{static}} \tag{3.37}$$

4. Motions of vessel
   This is an operational limit associated with experience rather than any physical limiting parameter. The roll and pitch of the Thialf must be small.

These limits are used to determine the operability.

Operability

The operability is based on the limiting criteria, the response spectrum and the wave spectrum. It defines the limiting combinations of significant wave height H_s and the peak period T_p for each wave direction and each limit. It is obtained from the limit and the response, as presented in Eq: 3.39.

$$Operability = \frac{Limit}{Response} \tag{3.38}$$

So per limit and for each (peak) period the maximum allowable significant wave height is determined.

$$H_{Smax}(T_p, dir) = \frac{Limit}{SMPM(T_p, dir)} \tag{3.39}$$

With the way to determine forces, the response from an equation of motion known and a way to gain more insight in the behaviour of the multi-body system an approach is made to choose which theory should be applied where to determine the forces on the different bodies.

3.5. Theory analysis

In this section the theory as presented in this chapter will be analysed. It will be determined how this theory is going to be used in this study and the reason why. First it must be determined which theory should be used to calculate the hydrodynamic loading on the bodies. The hydrodynamic loading on structures is composed of diffraction, inertia and drag forces. A way to characterise these forces is by the non-dimensional numbers like the KC number. Chakrabarti defined the different regions where different forces should be applied as described in Section 3.2.1.

To determine which forces are dominant and should thus be taken into account for the hydrodynamic loading first the Thialf and jacket dimensions should be defined. The width of a floater is 30m and the total length 201m as described in Table 3.3. The legs of the jacket are the thickest members with 2.2m in diameter and the risers are the thinnest members with a diameter of 0.3m. A sea state of 1m to 3m wave height and periods ranging from 4 seconds to 16 seconds is considered. The wave length is determined using Equation: 3.4. The results are summarised in Table 3.3.

Table 3.3: Dimensions Thialf and North Sea jacket.

	Thialf		**North Sea jacket**	
	min	max	min	max
D [m]	30	201	0.3	2.2
H_s [m]	1	3	1	3
T_p [s]	4	16	4	16
λ [m]	25	399	25	399

With the dimensions and the sea state the KC number, the equivalent KC number and the diffraction parameter π D/λ are calculated and reported in Table 3.4 and visualised in the Chakrabarti diagram in Figure: 3.10.

Table 3.4: KC Number and wave forcing parameters according to Chakarbarti [5].

	Thialf		**North Sea jacket**	
	min	max	min	max
KC	0.01	0.31	0.71	31
π D/λ	0.24	25	0.002	0.28
H/D	0.002	0.10	0.23	10

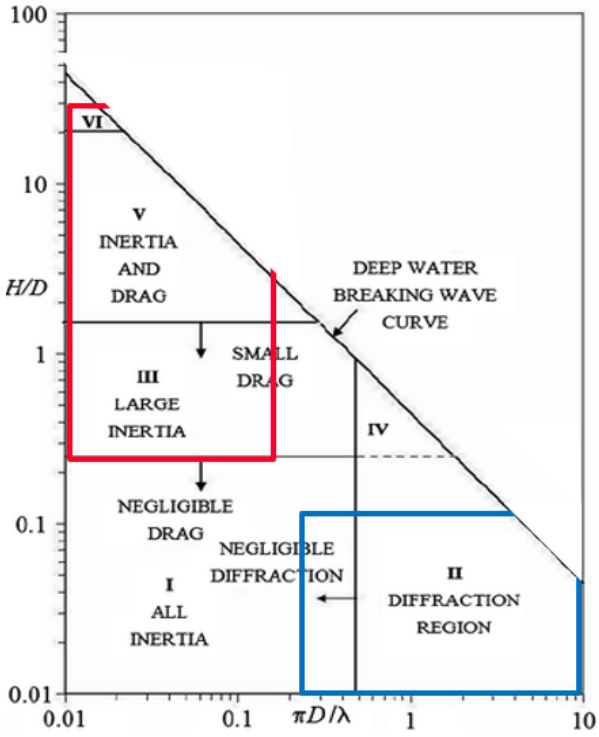

Figure 3.10: Thialf(blue) and Jacket(red) in the Chakrabarti diagram [5].

Out of the above mentioned it is concluded that the hydrodynamic loading on the Thialf is characterized by inertia and diffraction forces. And that the jacket is a slender body while it is characterized by inertia and drag forces (and thus diffraction is neglected). As stated in Section 3.3 it will be investigated if it is possible to solve the problem in frequency domain. And what the shortcomings and/or limitations are for determining the response in the frequency domain.

The Thialf hydrodynamic loading is going to be determined using diffraction theory as described in Appendix A. The hydrodynamic loading on the jacket is going to be determined using the Morison equation as given in Section 3.2.2. The waves are long compared to the diameter of the members, $\frac{\lambda_{min}}{D_{max}} = \frac{25}{2.2} > 5$ and thus Morison can be applied.

In this study it is assumed that the deep water approach can be used. With a water depth of 125 m [28] this means that the maximum deep water wave period can be 12.7 seconds. It should be noted that the waves with periods from 12.7s to 16s are intermediate waves but are treated as deep water waves. This means that the $tanh(kh)$ is actually 0.96 instead of 1 which is being assumed for the waves with a period of 16 seconds.

The marine growth effects the structure in three ways as described in Section 3.2.1. The surface roughness changes, the mass changes and the thickness changes. In this study the additional mass will be taken into consideration. Also the appropriate and inertia coefficients will be considered, for the drag coefficient a Reynolds number depended approach is chosen, but based on smooth members. An in-house Heerema study on the North Sea jacket by de Jong [10] showed that the effect of the increased diameter can be neglected as long as the rough member drag coefficients is used as recommended by DNV [41].

There are two issues while modelling the damping in the frequency domain.

1. The non-linear nature of the damping;
2. The relative velocity between the jacket hanging from the cranes and the waves.

In the frequency domain approach the quadratic damping term from the Morison equation must be linearised. The linearisation depends on the equivalent energy approach described by e.g. Clauss [6]. In this approach the amount of energy that is dissipated over a period must be the same for the linear and the non-linearised drag force.

For regular waves the velocity is $u(t) = u_a cos(\omega t)$. The drag related energy dissipated over a period for the linear, F_{DL}, and the non linear drag, F_D, must be the same.

$$E = \int_0^{2\pi} F_D \cdot u \cdot d(\omega t) = \int_0^{2\pi} F_{DL} \cdot u \cdot d(\omega t) \tag{3.40}$$

With the nonlinear drag: $F_D = \frac{\rho}{2} C_D D|u|u$

And the linear drag: $F_{DL} = \frac{\rho}{2} C_{DL} D u$

With the regular wave velocity and Equation: 3.40 we obtain:

$$C_D u_a^3 \int_0^{2\pi} |cos(\omega t)| cos^2(\omega t) = C_{DL} u_a^2 \int_0^{2\pi} cos^2(\omega t) \tag{3.41}$$

From this the linear drag coefficient can be found:

$$C_{DL} = \frac{8}{3\pi} C_D u_a \tag{3.42}$$

The linearised drag is thus:

$$F_{lineardrag} = \frac{\rho}{2} C_D D \left(\frac{8}{3 * \pi} u_a \right) u \tag{3.43}$$

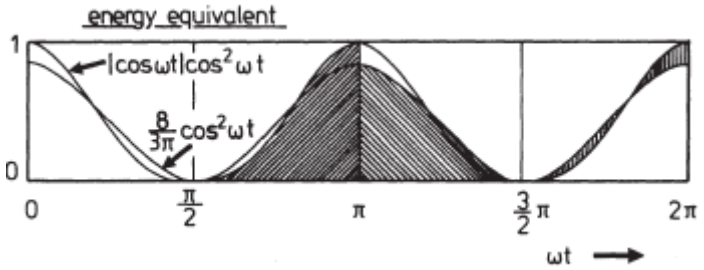

Figure 3.11: Equivalent energy drag linearisation [6]

The first problem of the frequency domain approach is solved, the drag is linearised. Now the second problem is elaborated on. The second problem is related to the relative velocity between the jacket and the waves. The jacket will oscillate due to the waves and the motion of the Thialf. The damping is mainly important near the natural frequencies, since the other terms cancel each other out, as described in Section 3.3. For the absolute velocity approach the drag due to the velocity of the jacket and the drag due to the wave are determined separately, this is described in Section 3.2.2. First the jacket is moved through still water with a jacket velocity $\dot{x}$, from this the damping force matrix, **B**, is derived. Then the jacket is fixed and waves are generated, from this the damping resulting from the wave velocity is determined for each frequency as a force vector, **F**.

To determine which kind of Morison equation approach to choose the resulting jacket velocity will be calculated first using the absolute velocity approach. From this it will be determined if this is the correct approach or not. As a part of this the DNV code will be consulted, although it should be noted that it is derived for current plus waves. If the relative velocity approach is necessary it will be investigated how this can be

implemented in the used software or otherwise be determined by an alternative approach. One should keep in mind that not only the relative velocity between the jacket and the waves is important here but also the relative velocity between the two legs. This differences is due to the phase difference w.r.t the wave between for the two legs (since there is a physical distance between them). Through the steps as described above the gap will be filled in.

To summarise the theory analysis, as stated above, the following conclusions are formulated:

- Airy linear wave theory for deep water will be used;
- The Morison equation will be used for the jacket;
- The Diffraction theory will be used for the Thialf;
- A Frequency Domain approach will be made considering the:
  - Non-linear damping in the Morison equation;
  - With the absolute velocity damping approach and the relative velocity damping approach.

The theoretical background, the analysis and selection of the theory provides a good foundation for the study that will be conducted in the next chapters. To get a better understanding of the behaviour of the jacket while it is free hanging from the cranes of the Thialf first a model will be made with the jacket in air. This model can be compared with measured data of the North Sea jacket campaign. This way the forces on the Thialf, determined with the diffraction theory, can be checked. If the model matches the behaviour of the measurements it can be expanded by submerging the jacket. Also the in air case will be used for comparison with the submerged jacket later on. The additional forces on the jacket will remain the only unknowns. This will be investigated in Chapter 5.

4

Base model

In this chapter the model of the crane suspended jacket decommissioning with the jacket hanging in air will be investigated. The measured data during the North Sea jacket campaign is compared to the model predictions (based on Heerema's current practice) of the free hanging jacket transport in air. It is the aim to determine how well the free hanging jacket motions are predicted by the model and whether it is thus a good starting point to expand the model with the jacket in water. First the Liftdyn model will be described. Secondly it will be explained how the measurement data was obtained and how it is used. And lastly a comparison between the measurements and the model is performed.

4.1. Model description

A model of the Thialf and the jacket is made in Liftdyn. Liftdyn is a in-house computer tool that is designed to model and solve general linear hydrodynamic problems in the frequency domain. Liftdyn can solve systems consisting of rigid bodies connected to each other or to the earth by springs, dampers and hinges. The body may have a frequency depended mass and damping, and frequency depended exciting forces resulting in a frequency depended response or RAO of the system. Due to the superposition principle the response is the sum of the responses that would have been caused by each body individually. This means that all different contributions that influence a multi-body system can be determined separately and then be added together to solve the whole systems response. The hydrodynamic properties for the Thialf are obtained via WAMIT for example, and are implemented in Liftdyn. For a more detailed description about Liftdyn and WAMIT, see Appendix B.1.

The Thialf is modelled as rigid body to which properties are assigned. The properties are given in Table **??** and a hydrodynamic database was imported. This database contains the coefficients for the added mass, damping, hydrostatic spring and the wave forces. The databases for the Thialf are derived by Heerema and are widely used within the company. The hoist wires are modeled as springs with a initial position and a stiffness and a pretension. The stiffness of the spring is defined with an axial stiffness EA with A the effective diameter of the sling/hoistwire and E the Young's modulus of the wire. The wires are under pretension to equal out to the static load of the jacket, which is elaborated on in this section. This means that environmental loads on the wires are not included. The spreaderbars and main hooks are modelled as rigid bodies. The spreaderbar on port side weighs 299 t, the spreaderbar on starboard weighs 346 t and the main hooks weigh 236 t each.

The jacket is also modelled as a rigid body which consists of various tubular structural members. The geometry of the jacket is approximated by a square jacket of which the properties match the real jacket and are presented in Table **??**. The coordinates of the center of gravity are given with respect to the center of the base of the jacket. The jacket that is shown in Figure: 4.1 is just for visualization with regards to the geometry. It has the correct height en width but the cross members and the diameters of the tubular members are not correct. But the center of gravity and the connection points to the hoist wires are in the correct location. And all the relevant properties are assigned with respect to the center of gravity of the jacket so the calculations can be performed in a correct way.

The global coordinate system is located at the stern of the Thialf, at the centerline of the keel. It coincides with the local axis system of the Thialf and is shown in Figure: 4.1a. With a right-handed axis system where the x-axis is positive towards the bow of the Thialf, the y-axis positive towards portside and the z-axis pointing upwards. The local coordinate system of the jacket is located at the center of the base. With the x-axis pointing upwards, the y-axis parallel to the global x-axis and the z-axis positive towards the top of the jacket.

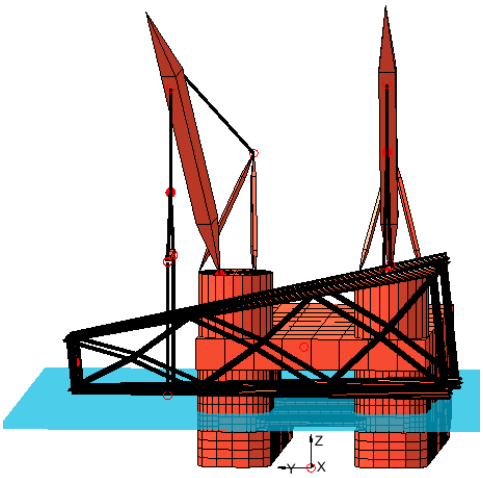

(a) View from the stern.

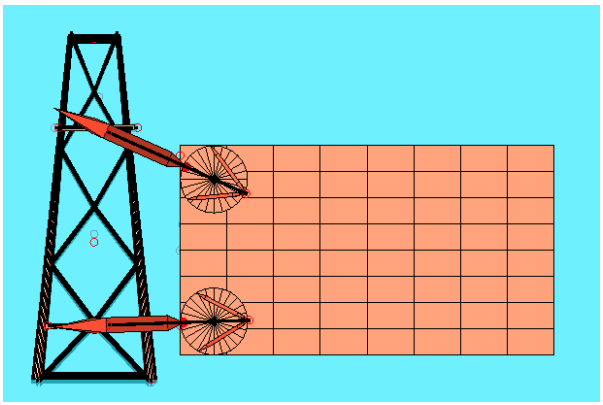

(b) View from above.

Figure 4.1: SSCV Thialf with the unrestrained crane suspended jacket [30].

The jacket is connected to the cranes by means of slings. For all these slings the pretensions needs to be determined so that the system is in static equilibrium, as stated earlier. It will later also be used to determine the DAF during the operability calculations. To determine the hookload a free body diagram was made, as shown in Appendix C. The hookloads need to be the same as the total weight from the jacket and the auxiliary equipment. With the hookloads and the sling configuration the required pretensions are determined and presented in Table 4.1. The stiffness of the spring is the axial stiffness EA with A the effective diameter of the sling and E the Young's modulus of the wire. And the angle is determined as the internal angle between the end of the sling and the beginning.

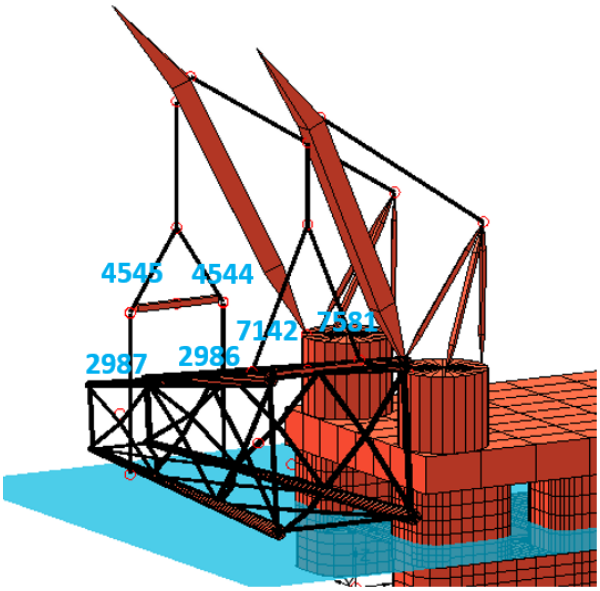

Figure 4.2: Sling configuration

Table 4.1: Pretension slings

	LP	Sling.No	Angle [deg]	Pretension [kN]
PS	1	SL 2987	90.00	12,949
	2	SL 2986	90.00	12,949
	3	SL 4545	56.71	17,247
	4	SL 4544	56.52	17,247
SB	5	SL 7142	65.88	20,368
	6	SL 7581	67.37	20,141

All the different aspects for the setting up of the equation of motion are described above. The general equation of motion, given in Equation: 3.28, will be filled in with the values and the hydrodynamic database specified above. This equation will be used to compile the RAO's, according to Equation: 3.29. In Equation: 4.1 it is shown which effects are included in the combined equation of motion. Where $\mathbf{M}_T$ is the mass matrix of the Thialf and $\mathbf{A}_{hyd}$ is the hydrodynamic (added) mass matrix of the vessel. $\mathbf{M}_J$ contains the mass matrix of the jacket that is hanging from the cranes. And $\sum_1^4 \mathbf{M}_{aux}$ contains the masses of the four other bodies namely the two spreaderbars and the two main hooks . The hydrodynamic damping from WAMIT for the vessel is specified in $\mathbf{B}_{hyd}$. To correct for the fact that the bodies are actually not completely rigid and since a minimum value of damping is required for asserting damping presence in all of the modes of the system a percentage of 0.3% of the critical damping for each mode is determined and added in $\mathbf{B}_{crit}$. $\mathbf{C}_{hyd}$ contains the hydrostatic spring terms of the vessel. The stiffness of the hoist wires that lift the jacket are represented in $\mathbf{C}_{wire}$. The motion of each body for each of the degrees of freedom can be determined with Equation: 4.2. $\mathbf{F}_{exc}$ is the sum of all the excitation forces. In this case this will consist of the wave excitation force on the vessel ,$\mathbf{F}_a$, which is determined in WAMIT.

$$\mathbf{S}(\omega) = -\omega^2 \cdot (\mathbf{M}_T + \mathbf{A}_{hyd} + \mathbf{M}_J + \sum_1^4 \mathbf{M}_{aux}) - i \cdot \omega \cdot (\mathbf{B}_{hyd} + \mathbf{B}_{crit}) + (\mathbf{C}_{hyd} + \mathbf{C}_{wire}) \tag{4.1}$$

$$\mathbf{x}(\omega) = \mathbf{S}(\omega)^{-1} \cdot \mathbf{F}_{exc} \tag{4.2}$$

Mode shapes and their natural period give a lot of insight in the behaviour of a model. They can be used to visualise what motions of the model are most important in different frequency regions. The mode shapes can be determined as explained in Chapter 3.1 with Equation: 3.3. The first ten mode shapes are presented in Table 4.2. Note that the motions are given w.r.t. the global coordinates (so not the local coordinates for the jacket). An additional spring matrix is defined for the Thialf to mimic the effect of the DP system and constrain the lowest three modes.

Table 4.2: Natural modes of the coupled Thialf-Jacket system

No.	Thialf	Jacket
1	Yaw	-
2	Sway	-
3	Surge	-
4	Roll	Sway in phase
5	Pitch	Surge in phase
6	-	Yaw
7	Heave-Pitch	Surge antiphase
8	Pitch Heave	Surge antiphase
9	Roll	Sway antiphase
10	-	Pitch

In Figure: 4.3 the RAO's obtained via Liftdyn are presented. In this figure the roll and pitch motion of the

vessel are given for incoming waves of 145 degrees. The wave frequency is on the horizontal axis. On the vertical axis the amplitude is given for each frequency. The colour under the curve has no influence here, only the outer line of the curve is of interest.

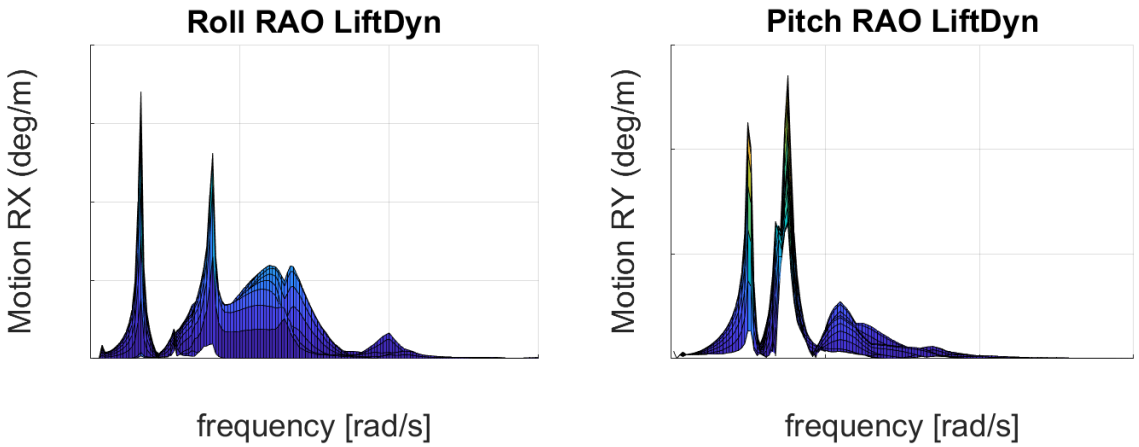

(a) Roll RAO for the Thialf with waves coming from 145 deg.

(b) Pitch RAO for the Thialf with waves coming from 145 deg.

Figure 4.3: Response amplitude operators of the vessel.

In Figure: 4.3a the peaks suggest that there are natural modes. The same holds for the two peaks in Figure: 4.3b. They match with the calculated modes from Table 4.2. For the pitch and the roll RAO the mode which is closed to the wave frequency range is visualised below. For the roll mode this is mode 9. In this mode the Thialf is rolling and the jacket is swaying out of phase with the Thialf. The visualisation is given in Figure: 4.4a . For the pitch mode this is mode 8. In this mode the Thialf is pitching and heaving and the jacket is moving in surge direction out of phase with the vessel. It is visualised in Figure: 4.4b. Note that the motions are exaggerated in the figures.

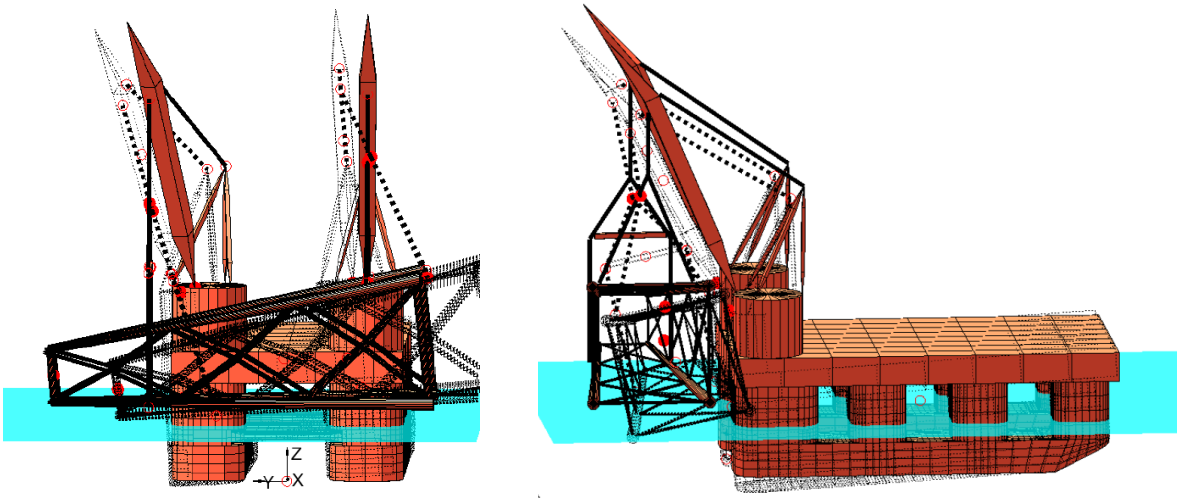

(a) Mode 9: Roll of the Thialf and surge of jacket in antiphase.

(b) Mode 8: Pitch of the Thialf and surge of jacket in antiphase.

Figure 4.4: Mode shapes 8 and 9.

4.2. Measurements

With the RAO's from the model known it is time to study the measurements that were performed. This will be done in the following order. First the measurement systems will be introduced, secondly the measurements of the motion are obtained and filtered. And thirdly the wave spectrum will be obtained from the wave-rider buoy.

On board the Thialf there are several monitoring systems installed and the collective term for all this equipment is Motion Monitoring Equipment#16 (MME16). There are systems to track the position of the Thialf, the crane loads, the power consumption and the motions of the Thialf. This systems were also used during the measurement campaign. The sensors that are used in this study are called Fiber Optical Gyroscopes sensors by Octan [14]. They record the vessel motion in six degrees of freedom, within 5cm or 0.01 deg of accuracy at a sample rate of 16 Hz[14]. It is used to determine the heading of the vessel and the roll and pitch of the Thialf. There was an additional measurement sensor installed on the jacket but unfortunately it did not work. Therefore only the Thialf motions are considered in this part.

The measurement campaign, from which the data is collected, started at 9.30 on May the 26^{th}. The jacket was lifted out of the water and the Thialf started the transport. The Thialf then started adjusting to the sail heading (150 deg), while simultaneously performed deballasting to the transit draf and connecting the bridal to the support tug. It sailed from the open sea to the more sheltered location in a fjord, at which the decommissioning yard is located. It arrived in the fjord on 27 May at around 17.00, so the total transit duration was about 29 hours. Afterwards, it sailed for 40 NM inshore along the fjord to the decommissioning yard.

A good window of the measured data must be selected, to make sure that there are no transient effects present since the model does not capture this. So a sufficiently long window was needed in which the vessel was still at the open sea but the heading, draft and the vessel speed are constant and the Thialf was not (de-)ballasting.

An adequate three hour window was found between 14.52 and 17.52 on the 26^{th} of May. The transient operations were completed and the the vessel was sailing in a constant direction and speed. More detailed output of the operation is given in Appendix C. The measured roll and pitch of the Thialf is presented in Figure: 4.5a. To make sure that the offset and the noise in the roll and pitch is not influencing the results a band pass filter has been applied. All the motions with periods above 60 seconds and below 2 seconds have been filtered out. Since the interest lies in the wave induced motions this is a valid assumption, motions outside that range are not induced by waves. The filtered motions are presented in Figure: 4.5b.

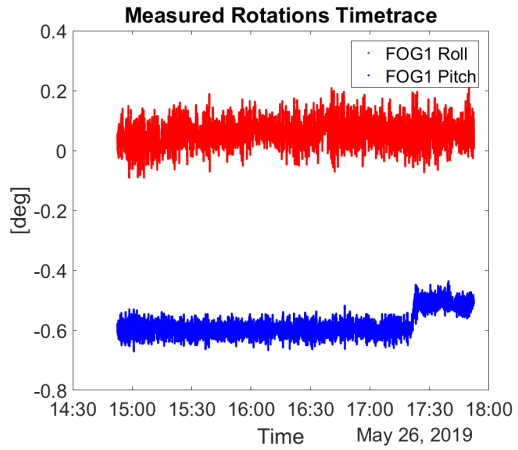

(a) Time trace of the Thialf roll(red) and pitch (blue) unfiltered.

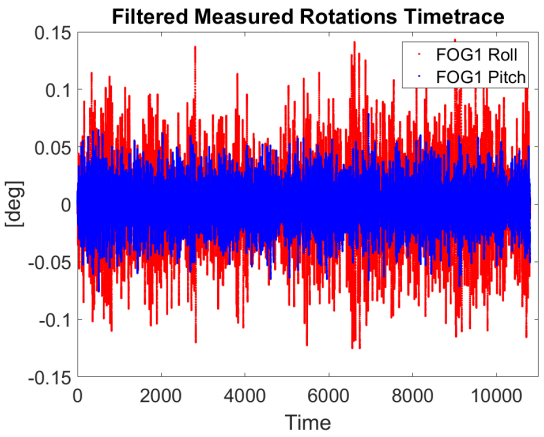

(b) Time trace of the Thialf roll(red) and pitch(blue) filtered.

Figure 4.5: Response amplitude operators of the vessel.

The filtered time traces are used to determine the spectral density. The spectral density describes how the energy of the time trace is distributed with frequency. The spectral density is calculated with the Fourier transform. The total amount of energy that is in the signal x(t) is transformed to $x(\omega)$:

$$\hat{x}(\omega) = \int_{t=0}^{t=10800} \exp(-i \cdot \omega \cdot t) \cdot x(t)^2 dt \tag{4.3}$$

And the spectral density can be defined as:

$$S_{xx}(\omega) = |\hat{x}(\omega)|^2 \tag{4.4}$$

The resulting spectral density for the roll and pitch motions of the vessel are plotted below in Figure: 4.6. With on the horizontal axis the frequency and on the vertical axis the spectral density in $(rad/s)^2 \cdot s$.

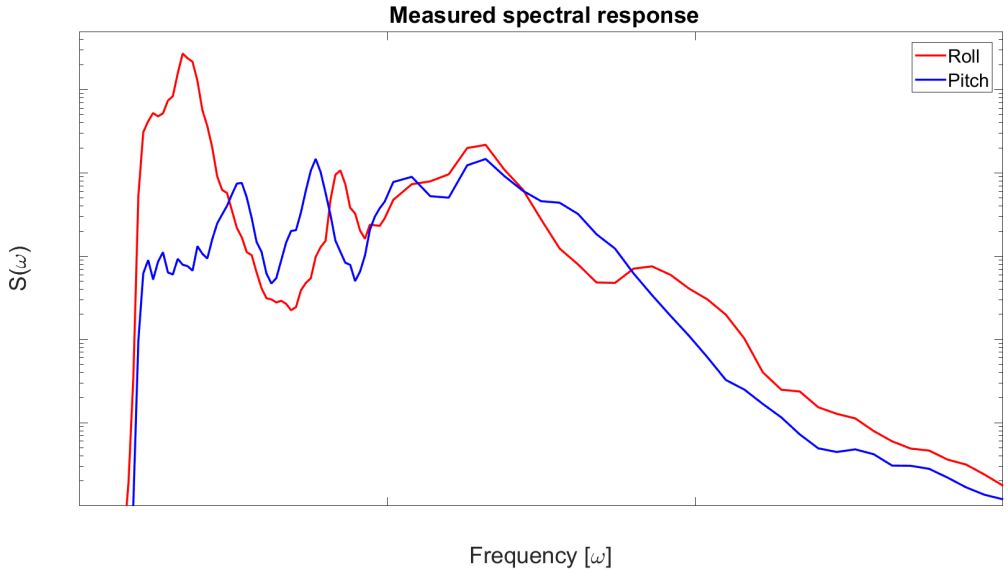

Figure 4.6: Spectral response of the measured roll and pitch.

To be able to compare the measurements to the Liftdyn model the wave spectrum is needed. A wave rider buoy was deployed near the original field. This wave buoy is fixed in one place. So the measured spectrum of the waves must be corrected for the fact that the Thialf is sailing with a certain speed in a given direction. The spectrum is corrected according to Journee [16] with a encounter frequency, as presented in Equation: 4.5. Where V is the vessel velocity and μ= wave direction relative to the ship's speed.

$$\omega_e = \omega - k \cdot V \cdot cos(\mu) \tag{4.5}$$

The vessel is sailing in almost the opposite direction of where the waves are coming from. As expected the energy of the spectrum shifts to the lower wave frequencies. It can be seen in Figure: 4.7 that there are mainly wind included wave and a small peak of swell waves in the lower frequencies. Now that the spectral response of the measured data is determined and the wave spectrum as well, it is time to determine the spectral response with of the model with the wave measurements and the RAO's from Figure: 4.3. Afterwards these two can be compared. This will be done in the next section.

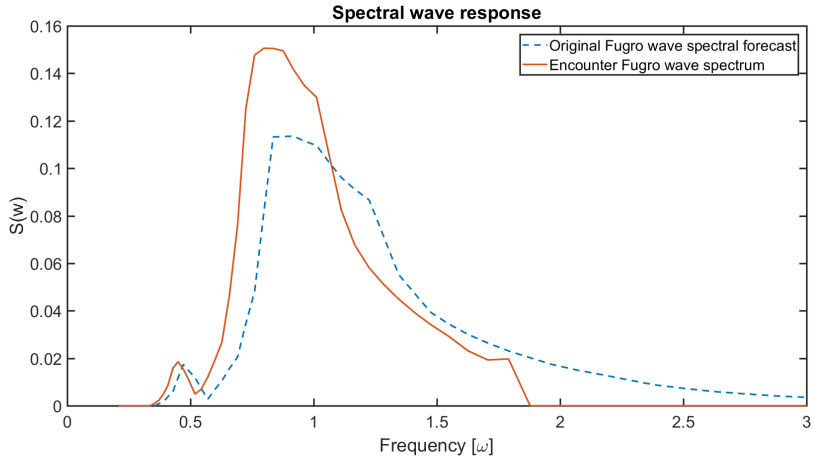

Figure 4.7: Measured wave spectrum and the corrected wave spectrum.

4.3. Measurements vs Liftdyn model

In this section the model predictions for roll and pitch will be compared to the measured data. To check if information got lost in translation from the time traces to the spectral response and the filtering the significant double amplitude (SDA) will be determined for each case.
The spectral roll response is determined and shown in Figure: 4.8. With the measured spectral response (in red) and the modelled spectral response from Liftdyn, derived by the RAO from Liftdyn and the measured (encounter) wave spectrum (in black). The natural frequency of mode 9 is highlighted with a dotted red line. The spectral pitch response is shown in Figure: 4.9. With the measured spectrum in blue and modelled spectral response from Liftdyn (in black), derived by the RAO from Liftdyn and the measured (encounter) wave spectrum. The natural frequency of mode 8 is highlighted with a dotted red line.

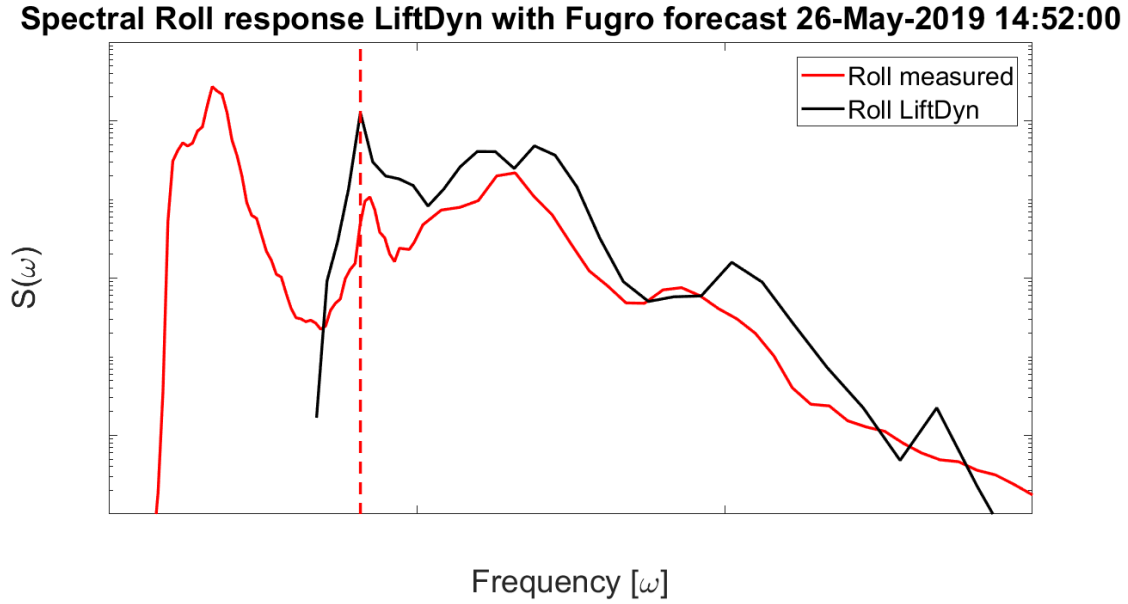

Figure 4.8: Spectral roll response for the Thialf with waves coming from 150 deg.

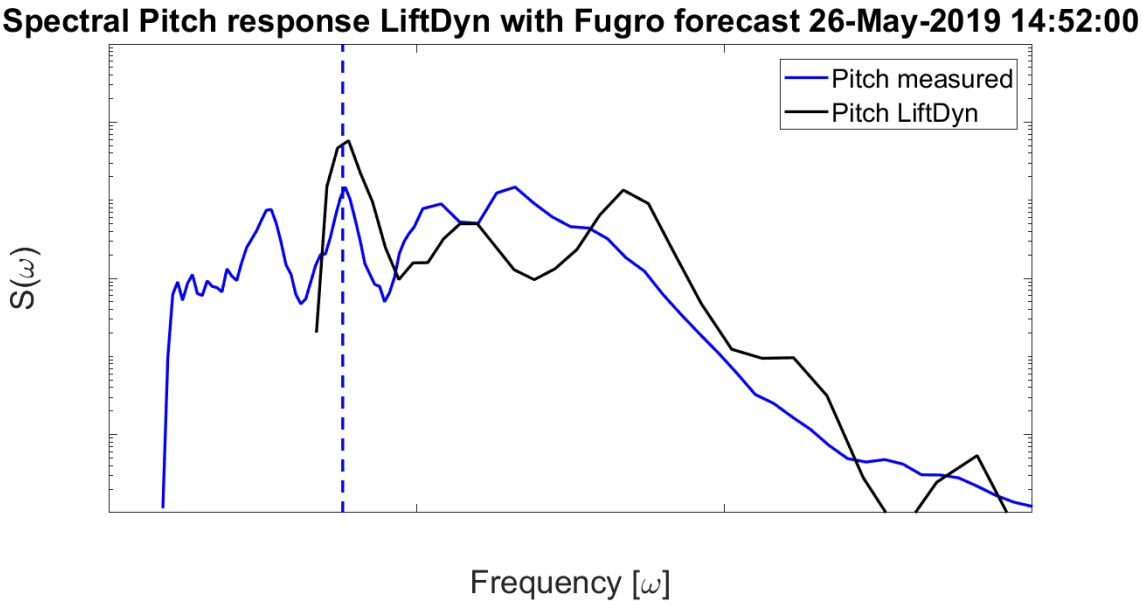

Figure 4.9: Spectral pitch response for the Thialf with waves coming from 150 deg.

The SDA can be calculated according to Equation: 3.35 in the frequency domain. For the time trace the SDA was calculated based on the standard deviation, σ, as:

$$SDA_{tt} = 4\sqrt{\sigma^2} \tag{4.6}$$

The SDA is calculated for four cases, the unfiltered time trace measurements (1), the filtered time trace measurements (2), the filtered spectral response from the measurements (3) and the calculated spectral response(4). The results are presented in Table 4.3.

Table 4.3: Significant double amplitudes for roll and pitch.

Case	**Roll SDA [deg]**	**Pitch SDA [deg]**
1. Unfiltered	0.174	0.15
2. Filtered tt	0.159	0.076
3. Filtered FD	0.157	0.077
4. Calculated	0.143	0.088

Based on the results in this chapter the following observations are made and conclusions are drawn. The weather was very good during the transport. This resulted in very low amplitude motions.

The model predicted the natural modes and the trend well. There is a very small offset when comparing the natural peaks from mode 8 and mode 9 in Figure: 4.8 and 4.9. The models do seem to underestimate the damping in the antiphase modes since both of the calculated peaks are higher. This could be due to the (double) pendulum motion of the jacket that is moving out of phase with the Thialf, but since the sensor on the jacket did not work this is hard to verify.

When looking at the effect of filtering and processing the data the SDA was used. It can be seen that the overall amplitudes where quite low, around 0.08 deg for pitch and 0.15 deg for roll. Where the limit was set to 1 deg for both pitch and roll. Most of the energy that was discarded during the process was in the filtering of the pitch data, where the SDA is almost halved. This is due to the jump offset from around -0.6 deg to -0.45 deg of the pitch.

In the low frequency part, there was no wave energy measured by the wavebuoy but a response was measured by the sensors. Therefore there is no energy in the modelled response but there is in the measurement response. When looking at the frequencies of the roll peak and the pitch peak they do match with Thialf heave-pitch - jacket surge in phase, mode 7, and the Thialf roll - jacket sway, mode 4. The roll motion of mode 4 is not likely triggered by waves due to the low frequency, it is expected that it is caused by DP induced motions.

Concluding this chapter, the Liftdyn model with the Thialf and the jacket is a good starting point to expand the model and investigate what happens if the jacket is lowered through the waterline. In the next chapter it will be investigated what influences should be added to the jacket once it is in the water.

5

Submerged Jacket Model

In this chapter a methodology is set up to determine relevant forces and the resulting motions while having the crane suspended jacket (partly) into the water. The frequency domain model from the in air case is updated by partly submerging the jacket. The model and the hydrodynamic database for the Thialf is already known from the previous chapter. But for the jacket the model and hydrodynamic database has to be determined first. As a start the commonly used approach and method of HMC, with commonly used software, tools, and codes will be used. Then an alternative method for the software use and approach is made, with the aim to solve it in the frequency domain. First the model description is given. Then the different contributions are added to the jacket. After that a new approach is derived. Lastly a case study is performed where different parameters are varied.

5.1. Model description

The model from the in air case is used as a starting point. The jacket will be lowered in to the water. For the Thialf the model and the data is already available. But for the jacket the added mass, damping and wave forcing on the jacket have to be determined. As a start the commonly used approach of HMC, with commonly used software, tools, and codes will be used. This is visualised in Figure: 5.1.

The forces on the jacket can be determined with the Morison equation and will be linearised so they can be used in the frequency domain as explained in Section 3.5. To be able to determine the forces on each of the members the exact geometry of the jacket is needed. This geometry and weight distribution is modelled in SACS, see Appendix B.1 for more information on SACS. The jacket is presented it Figure: 5.2, for clarity the open members are visualised in red and the closed members are in yellow. The two legs and the associated pile sleeves on the upper part of the jacket in the figure are open. The two legs on the bottom of the figure are capped at the top of the jacket (left side of the picture, at the side where the topside was located). Also the auxiliary pipes are open, like the caissons for example. The SACS model is then converted to a Moses model in which the hydrodynamic loads will be determined for the jacket. In this database the hydro statics, Morison damping and added mass and wave forcing will be derived based on the absolute velocity approach as described by in Section 3.2.2. The loads calculated in Moses will be adapted to make a hydrodynamic database via Excel so it can be used in Liftdyn. Since the damping is nonlinear it will be linearised with the equivalent energy approach described in Equation: 3.40. For the Thialf the hydrodynamic properties are taken from the Wamit, in the same way as described in Chapter 4.

Via Liftdyn the RAO's and responses are calculated, but an iteration is now needed with Moses. The initial jacket velocity that was used to determine the jacket damping matrix was based on an estimated guess. So the process will be iterated until the jacket velocity is converged. Then the results are post processed with Matlab.

Assumptions: As described in the scope wind and current are not considered in this study.

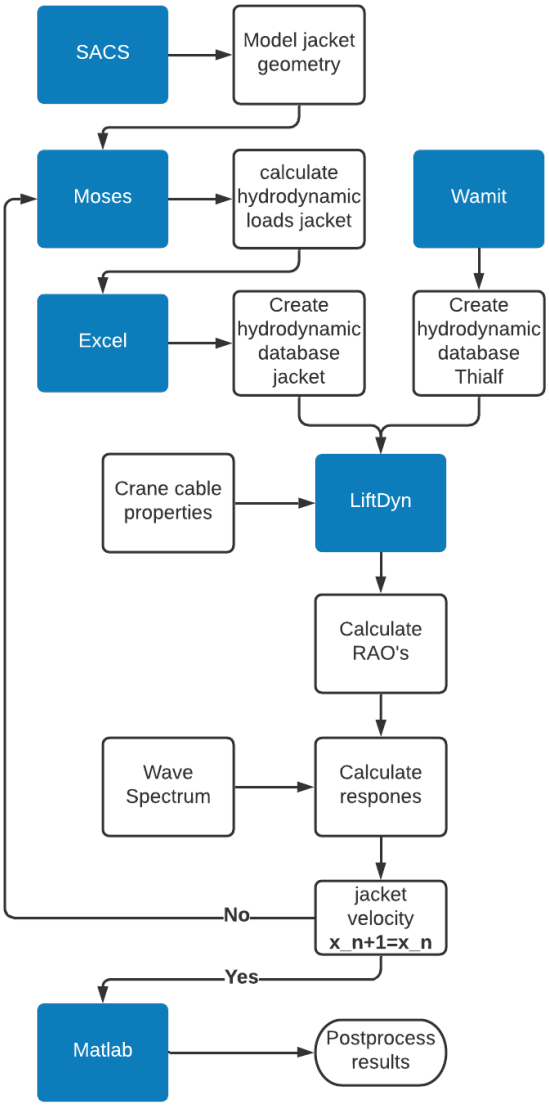

Figure 5.1: Flowchart approach

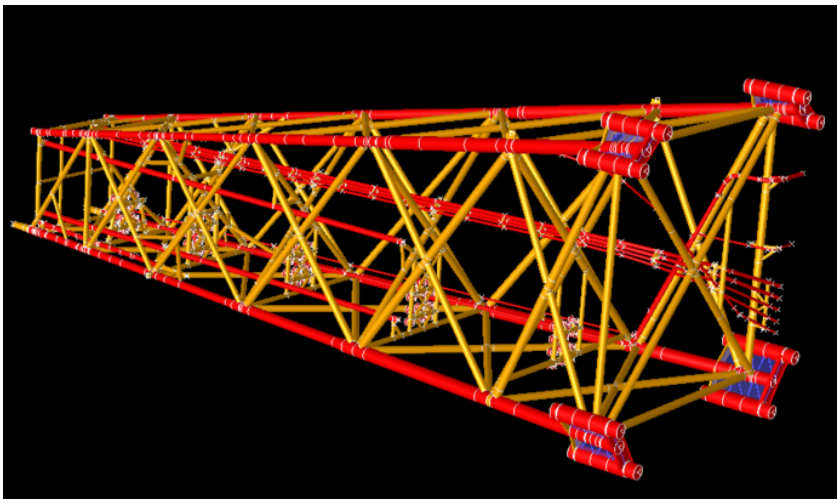

Figure 5.2: The jacket modelled in SACS [38].

5.2. Adding influences on the jacket

With the approach explained in the previous section the additional influences on the jacket will be determined in this section. First the effect of having the jacket lowered on the RAO will be investigated and the hydrostatic terms are determined. The added mass and the damping due to the jacket motions will be calculated. And lastly the wave forcing on the jacket, which consists of the added mass and damping due to the wave particle velocity will also be treated. The different effects due to the now partly submerged jacket will be elaborated next. In this study waves from behind will be considered (0 degrees).
Keep in mind that only the effects on the jacket are added one by one here. The effects on the Thialf, such as wave forcing, are present in all the cases treated here!

5.2.1. Static effects

Three static effects are investigated here, firstly the effect of lowering the jacket, secondly the effect of buoyancy and thirdly the hydrostatic stiffness.

Effect of lowering jacket

The jacket is lowered sufficiently deep so the bottom legs of the jacket stay submerged. Therefore the jacket is lowered 20 meters down from the original position (as used in Chapter 4). The bottom legs are now 8.65m under the still water level, as visualised in Figure: 5.3. By lowering the jacket into the water the sling length of the hoist wires is increased by 20 meters. Due to this longer length the pendulum motion of the jacket will also shift to a slightly higher period.

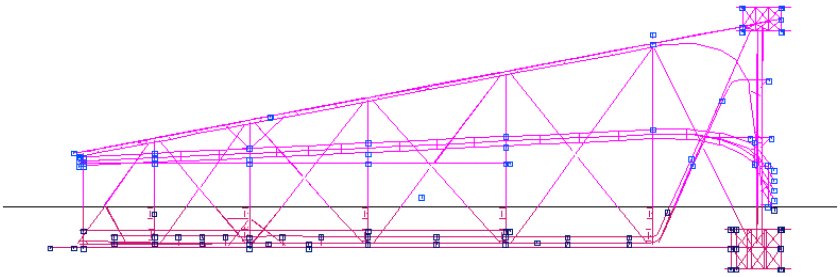

Figure 5.3: Side view of the jacket 8.65m submerged.

Buoyancy

Since the jacket is now partly submerged it will have buoyancy. In Figure: 5.2 it was shown which members are open (red) or are closed and thus filled with air (yellow). The total buoyancy is a combination of the entrapped air and the displaced water due to the submerged structural volume. The total buoyancy force of the jacket is 1330 t. This leads to a weight reduction on the cranes since the load due to the jacket reduces from 5959 t to 4629 t, this is a reduction of 22%. Since the hookloads reduce the pretensions on the slings also reduces. They are determined in the same way as described in Section 4.1, but now with the buoyancy included.

Table 5.1: Pretension slings submerged jacket.

	LP	Sling.No	Angle [deg]	Pretension in air [kN]	Pretension 8.65m sub [kN]
PS	1	SL 2987	90.00	12,949	8,152
	2	SL 2986	90.00	12,949	8,152
	3	SL 4545	56.71	17,247	11,507
	4	SL 4544	56.52	17,247	11,507
SB	5	SL 7142	65.88	20,368	17,156
	6	SL 7581	67.37	20,141	16,964

Hydrostatic stiffness

The hydrostatic stiffness matrix describes how the buoyancy (and weight) loads on the jacket change due to (small) changes in the jacket position and orientation. The hydrostatic stiffness components are only specified for the heave, roll and pitch degrees of freedom; for the other degrees of freedom of the jacket they are zero. The matrix is presented in Table 5.2.

Table 5.2: Hydrostatic stiffness of the jacket w.r.t. the center of buoyancy in kN/m.

	Heave	**Roll**	**Pitch**
z	**5.11E+02**	1.11E+03	6.61E+01
rx	1.11E+03	**1.04E+06**	9.67E+03
ry	6.61E+01	9.67E+03	**1.17E+05**

The effects of lowering the jacket and the static effects due to the submerging are presented in Figure: 5.4. In this figure the relevant motion RAO's of the jacket with waves coming from behind(0 deg) are presented. The following motion are considered and defined in the same direction as in Chapter 4.1: a) Surge, horizontal motion inline with the Thialf b) Heave, the vertical motion and c) Pitch, rotation towards the Thialf. The RAO's of the Thialf and the other motions of the jacket are summarised in Appendix D.1. On the horizontal axis are the different periods and on the vertical axis the response per meter wave height. Before going in on the different contributions it can be seen that there are two distinctive peaks in the figures. One peak at a high period and one at a low period. These peaks correspond with mode 8 and 10 from Table 4.2 and are the Pitch-Heave of the Thialf with jacket surge antiphase and pitch of the jacket respectively. Looking at the motions of the jacket in air corresponding with the 8^{th} mode (high period peak)) it can be seen that the jacket is also following the motion of the Thialf for heave and is also pitching while slinging back and forward in Surge direction. When comparing the RAO's of the jacket in air with the ones where the jacket is lowered (but the effects of the water are not included) it can be seen that the peak from mode 8 shifts to a higher period, as expected for a longer sling length. It also amplifies a new mode, mode 11 surge of the spreaderbar on port side. By adding the static effects of buoyancy and the stiffness mode 11 is reduced significantly in amplitude. But the jacket pitch, mode 10, is triggered due to the low stiffness in pitch direction. The stiffness is sufficient to reduce height of the peak at the higher period for surge and pitch. By lowering the jacket and adding the static effects the Thialf is only affected at the higher period modes, but less severe than the jacket, see Appendix D.2.

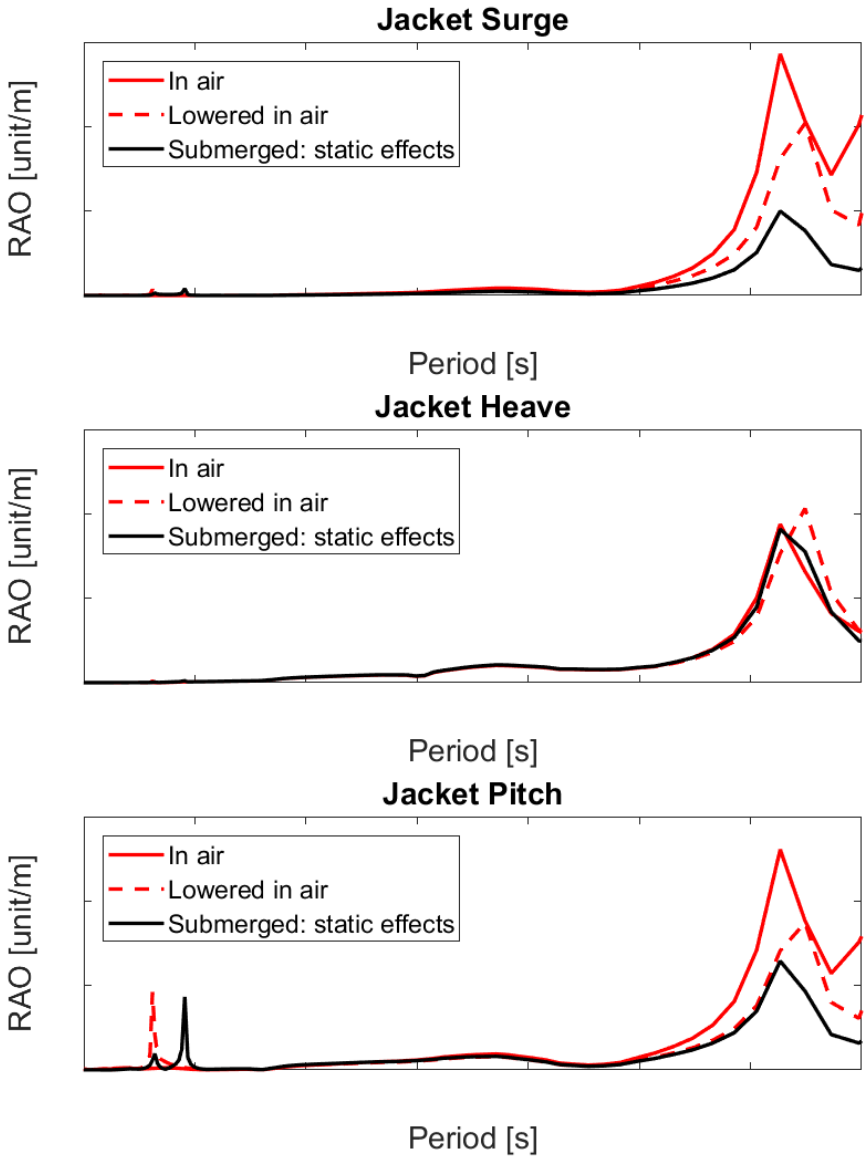

Figure 5.4: Influences on the jacket due to static effects.

5.2.2. Hydrodynamic effects

After analysing the effects of having the jacket lowered and the (hydro-)static effects the hydrodynamic effects are investigated. First the different components are discussed after which the effects on the jacket RAO's are discussed. Remember that the effects on the jacket are added step-by-step but the forces on the Thialf are all present.

Added mass

The added mass is a combination of the due to the water that is in the flooded members and the Morison inertia terms. For each member the inertia terms is determined according to the Morison Equation: 3.16 presented in the equation below. And for the flooded members the entrapped water mass is added to the added mass matrix. The resulting added mass matrix is given in Table 5.3. It can be seen that the added mass in surge and heave direction are in the same order of magnitude, and they are about 60% of the mass of the jacket. The added mass in sway direction is much less than surge and heave, this is as expected as most members are in line with this direction and thus do not contribute to the added mass.

$$F_{M_{Inertia}} = \frac{\pi}{4}\rho D^2 C_m \ddot{x} \tag{5.1}$$

Table 5.3: Added mass matrix of the jacket w.r.t the center of buoyancy in t.

	Surge	**Sway**	**Heave**	**Roll**	**Pitch**	**Yaw**
x	**3.54E+03**	6.70E+00	-1.46E+01	1.00E+03	2.02E+03	7.61E+04
y	6.70E+00	**9.67E+02**	-1.25E+00	8.44E+02	-1.75E+01	1.91E+02
z	-1.46E+01	-1.25E+00	**3.61E+03**	-6.69E+04	-2.83E+01	-9.86E+02
rx	1.00E+03	8.44E+02	-6.69E+04	**8.52E+06**	1.24E+05	4.83E+04
ry	2.02E+03	-1.75E+01	-2.83E+01	1.24E+05	**1.31E+06**	1.76E+05
rz	7.61E+04	1.91E+02	-9.86E+02	4.83E+04	1.76E+05	**9.03E+06**

Wave force

The wave forcing on the jacket is caused by the water particle kinematics around the structure. From the waves the velocities and accelerations perpendicular to a member cause a drag and inertia component. The forces are calculated according to the Morison absolute velocity approach equation. The wave forces are calculated according to Equation: 3.22.

$$F_{M_{Wave}} = \sqrt{(\frac{\pi}{4}\rho D^2 C_m \dot{u})^2 + (\frac{\rho}{2} C_D D|u(t)|u(t))^2} \tag{5.2}$$

The resulting forces are summed in surge, sway and heave direction and give a resulting force (and a phase angle w.r.t. to the wave) for each period and each direction. The forces are multiplied with their horizontal and vertical positions w.r.t. to the center of buoyancy for the resulting moments in roll, pitch and yaw direction. The resulting surge and sway force are given in Figure: 5.5. The other directions are given in Appendix D.5. The forces and moments are used in the right-hand side of the equation of motion, as given in 4.1, as an excitation force to the system.

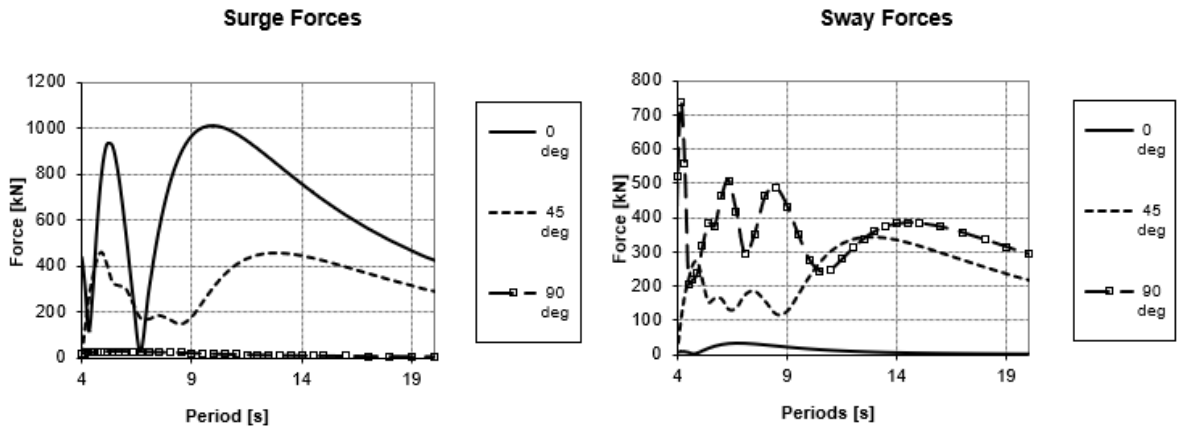

Figure 5.5: Wave force per meter wave height in horizontal directions on the jacket.

Damping

The damping due to the jacket velocity is obtained via the absolute velocity approach of the Morison equation. It is therefore treated as if the cylinder is oscillating in still water to the determine the jacket damping. This is done accordingly to the damping part of Equation: 3.18 which is linearised and is presented in Equation: 5.3.

$$F_{M_{Damping}} = \frac{\rho}{2} C_D D |\dot{x}| \dot{x} = \underbrace{\frac{\rho}{2} C_D D \frac{8}{3\pi} \dot{x}_a}_{Damping\ coefficient} \cdot \dot{x} \tag{5.3}$$

The damping coefficients matrix is obtained via iteration in Liftdyn and Moses, as explained in Figure: 5.1. The damping is linearised around the jacket velocity amplitude. Therefore the velocity is needed as input for determining the damping coefficients matrix. Thus an iteration is needed until the jacket velocity is converged for a given period and a direction, and the damping is linearised around the right value. The matrix presented here is obtained by iterating the jacket velocity (for all six degrees of freedom) around the low period peak and 0 degrees wave heading. It can be seen that the damping in sway is much less than the damping for surge and heave in this case, this is as expected since the jacket is barely moving in sway when the waves are coming from behind. It is also noted that the damping in pitch is about 2.5 times smaller than the damping in the other rotational directions. This is in line with the expectations since the arm over which the jacket rotates is much smaller in this direction compared to rotating it in yaw or roll direction.

Table 5.4: Damping coefficients matrix w.r.t. center of buoyancy in kN.s/m and kN.m.s./rad.

	Surge	**Sway**	**Heave**	**Roll**	**Pitch**	**Yaw**
x	**1.59E+02**	0.00E+00	2.55E-01	7.48E+00	1.71E+01	-1.71E+03
y	1.74E+00	**8.49E+00**	2.55E-01	3.74E+01	-1.03E+01	-5.72E+00
z	1.00E+00	0.00E+00	**1.02E+02**	8.83E+02	-1.31E+02	-8.58E+00
rx	1.70E+01	0.00E+00	1.10E+02	**2.63E+05**	2.90E+03	-8.58E+02
ry	1.89E+01	0.00E+00	0.00E+00	3.37E+03	**1.06E+05**	-2.00E+03
rz	-7.13E+02	0.00E+00	0.00E+00	-7.48E+02	1.42E+03	**2.84E+05**

With all the different dynamic contributions for the jacket determined they are now added one by one to the RAO's calculations. The results are in Figure: 5.6, where the jacket RAO's of the surge, heave and pitch are presented again. As a starting point the RAO's from the submerged case with the static effects from Figure: 5.4 are used, with the static effects denoted with the black line and the "S". First the added mass is added to the system, denoted with the blue line and the "A". Due to the added mass the natural frequencies shift to higher periods, as expected from natural frequency Equation: 3.32, a higher (added) mass leads to higher natural periods. And when looking at the surge motion of the high period mode the peak reduces in height due to the added mass. The mass is increased but there is no extra force present and thus the acceleration of the jacket, and the resulting motion reduces. Next the wave force on the jacket, denoted with the red line and the "W", is added. It can be seen that the wave force mainly influences the first peak, the pitch of the jacket mode. The natural period of the pitch mode almost coincides with the peak in wave force for pitch as well as surge. Outside this peak the influence of the wave force on the RAO's is small. Lastly the damping due to the jacket velocity, denoted with the green line and the "D", is added. It can be seen that the damping, that is linearised around the velocities of the pitch peak, mainly has an effect at the pitch peak. It damps the heave motion almost completely and the pitch and surge RAO significantly. The effect outside this peak is very limited, as it only slightly reduces the high period peak.

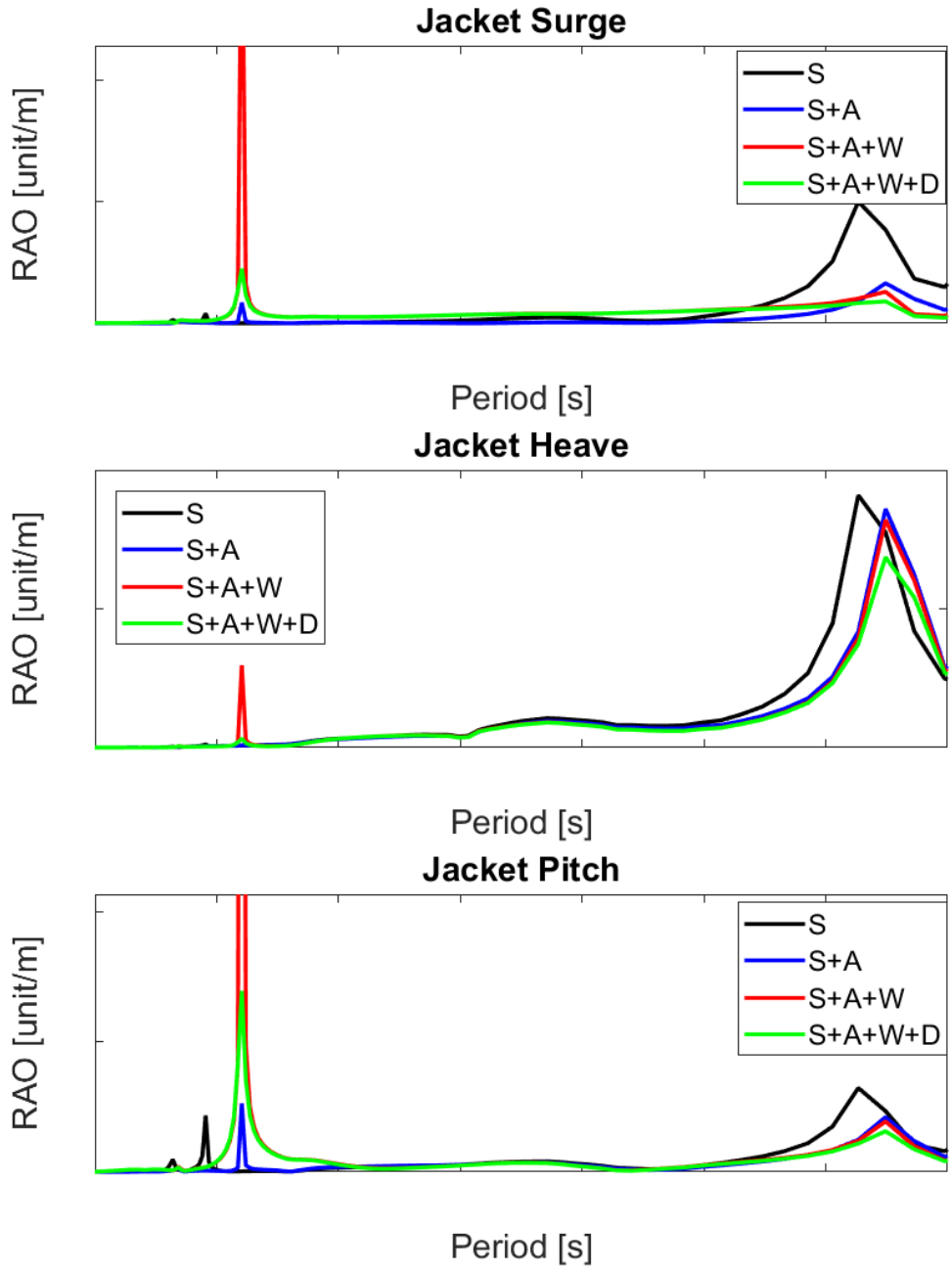

Figure 5.6: Influences on the jacket due to dynamic effects. With S the (hydro)static effects, A the added mass, W the wave and D the damping.

5.3. Relative velocity approach

In this section another approach to determine the damping on the jacket is investigated. First it will be explained why this has been done. Then the new approach will be elaborated on. After which the results and the findings are presented.

In the approach explained in the previous section the standard way of working with the tools and programs from Heerema is used. The absolute velocity approach was used to calculate the damping due to the jacket velocity and the wave particle velocities separately. In Section 3.2.2 it was shown that the damping can also be determined with the relative velocity approach, which uses the relative velocity between the waves and the jacket to determine the damping. This might be a more realistic approach. Since the damping scales with the velocity squared a different velocity could lead to a factor of four difference in the resulting damping. As seen in Figure: 5.6 the damping has a major impact on the response of the jacket near the pitch mode. When looking at waves from 0 deg, the jacket velocity in surge direction is in the same order of magnitude as the wave particle velocity (according to linear wave theory with 1m wave height at the low period peak). The wave particle velocity is 0.52 m/s at still water level and it decreases to 0.21 m/s at the bottom of the jacket. Therefore a new approach is set up to capture the influence of relative velocity while calculating the damping in the frequency domain. Since this approach is not affecting the other effects such as added mass and stiffness they are not further elaborated on here.

There are two things to keep in mind here concerning the relative velocity. Firstly, there is a relative velocity between the jacket motion and the wave. Secondly, there is a difference in relative velocity between the first and the second legs due to the physical distance between them. Since Moses can only output one wave force (and phase) per period and dampings matrix per body the model is cut into three parts. This way the relative velocity w.r.t. to the wave can be determined for each part. And the spatial difference is automatically taken into consideration since it is modelled by three parts, the front leg, the back leg and the middle part. The relative velocity between the wave and the jacket is captured by calculating the damping based on the relative velocity instead of the two separately. This velocity is obtained by iterating the relative velocity until in is converged. This is done via the following approach.The three parts of the jacket are presented in Figure: 5.7.

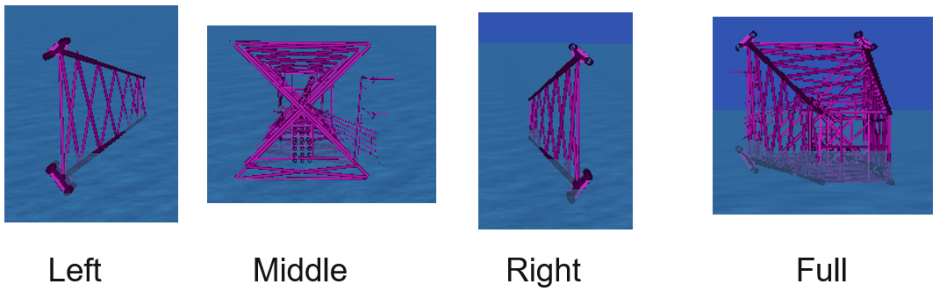

Figure 5.7: The jacket in three parts and the whole jacket.

The damping forces on the jacket is obtained as described in Figure: 5.8 per part. The damping matrix is determined by Moses and divided by the relative velocity. This coefficient matrix $\hat{B}$ will be used to determine the damping. For each of the three parts a different damping file (hydrodynamic database) is made. This database consists of a frequency depended ,linearised, damping matrix and a linearised, frequency depended, wave damping force. After linearising the damping around the relative velocity the damping can be split in two parts:

$$F_{M_{Rel}} = \frac{\rho}{2} C_D D|u - \dot{x}|(\dot{x} - u) = \frac{\rho}{2} C_D D(\frac{8}{3 \cdot \pi} r_a)(\dot{x} - u) \tag{5.4}$$

Which can be split in a part related to the jacket velocity and a part related to the wave velocity.

$$B_{damp} = (-\frac{8}{3 \cdot \pi})\hat{B} \cdot r_a \dot{x} \tag{5.5}$$

$$F_{wave_{damp}} = (\frac{8}{3 \cdot \pi})\hat{B} \cdot r_a \cdot u_{wave} \tag{5.6}$$

The three different parts are connected to a dummy body of the jacket by a joint which slaves the motions of the parts to the dummy. But via the joint the forces and moments from the different parts are transferred correctly to the system. This dummy body contains a hydrodynamic database with the mass, added mass, stiffness and wave inertia force. Each of the parts contain a damping file with a damping coefficients matrix and a wave damping force, based on Equations: 5.5 and 5.6 respectively.

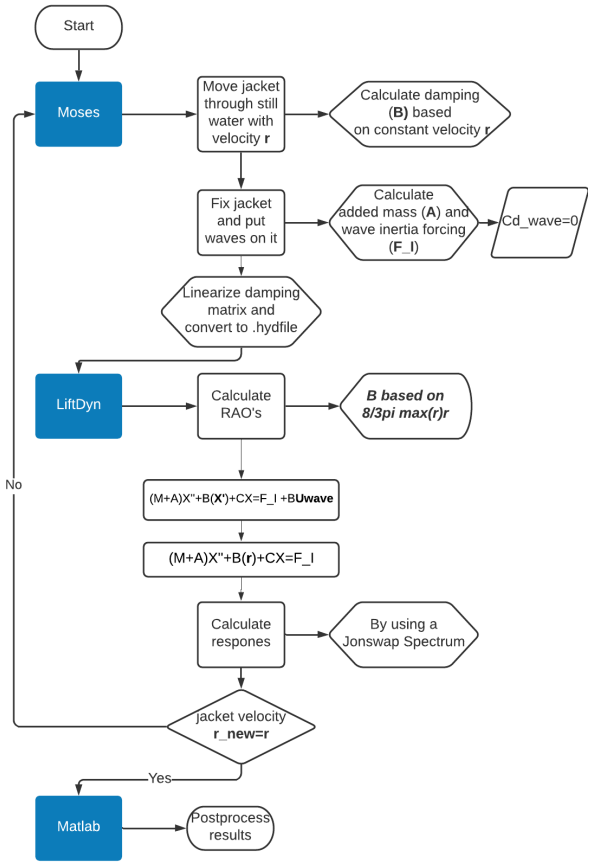

Figure 5.8: Flowchart relative velocity damping approach.

The procedure to determine the B_{damp} is similar to the way the damping coefficients matrix was determined in Section 5.2.2 only the relative velocity is now used to linearise around and for the velocities in x,y and z direction. For rx, ry and rz the jacket velocity was used since the wave velocity is described by a velocity component in x and in z direction (with waves from behind). For the wave damping the velocity in x and z is used based on linear wave theory. It is assumed that the wave force in all other directions is zero.

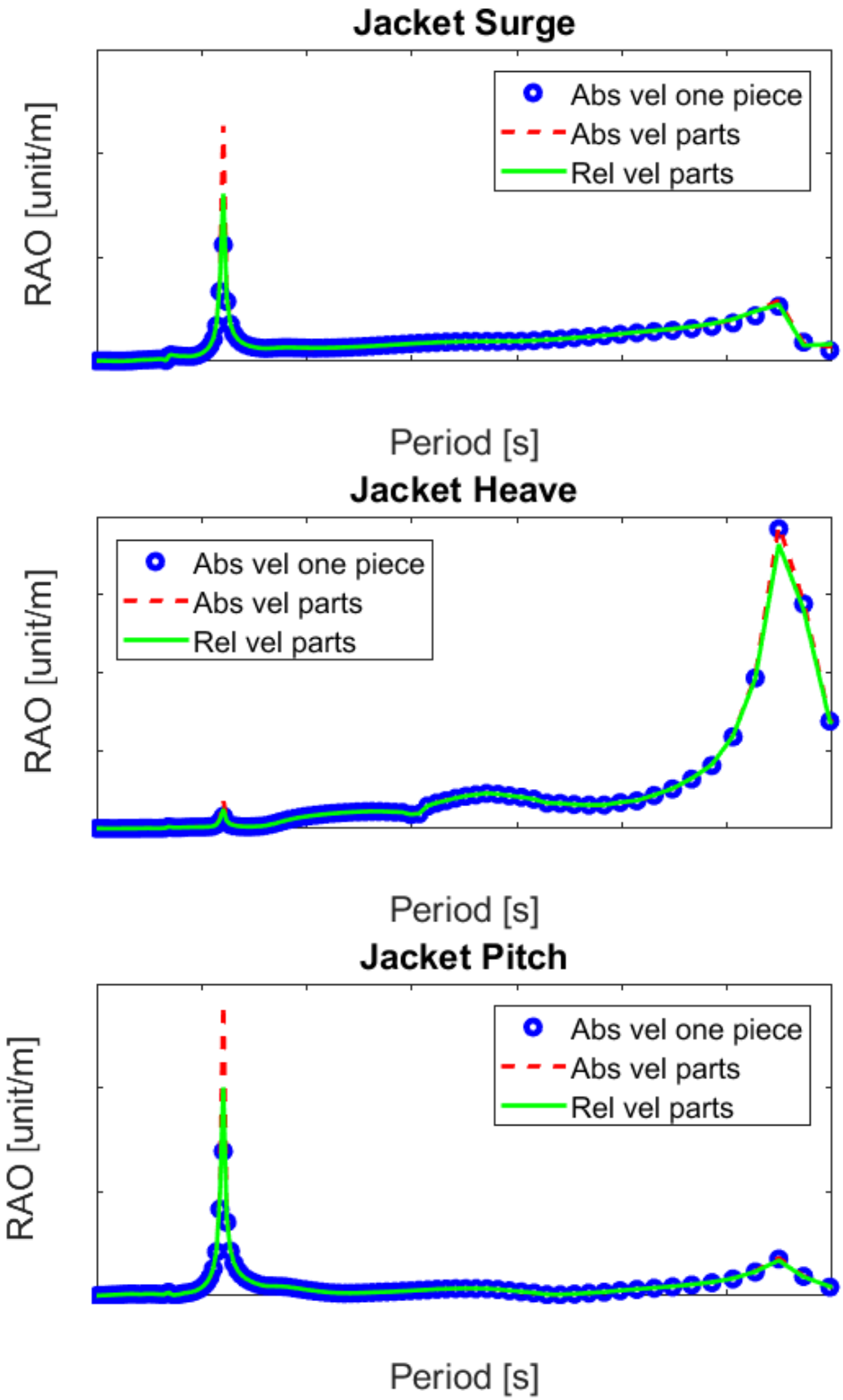

Figure 5.9: Jacket motions RAO with relative velocity approach

It can be seen from Figure: 5.9 that by modelling the jacket in parts the damping decreases near the jacket pitch peak. Since this mode is highly undamped, a slight change could lead to a large change in response. But when comparing the response from the absolute velocity approach by parts with the relative velocity approach by parts it is noted that the peak of the pitch mode is reduced by almost 30 %. Since the difference between cutting the jacket in three parts compared the jacket in one piece ('full') is already large for the absolute velocity approach, the relative velocity approach is not used for the rest of this study.

5.4. Case study

In this section a case study will be performed on the North Sea jacket. A different configuration with tugger winches and a different submerged depth will be investigated to study the effects on the two dominant modes as presented in Figure: 5.6. This will be done using the absolute velocity approach as presented in Section 5.2.

Submerged depth

A difference in submerged depth is investigated. The jacket is lowered another 10 meters and is now 18m submerged. At this depth the top legs are just above the water, as seen in Figure: 5.10.

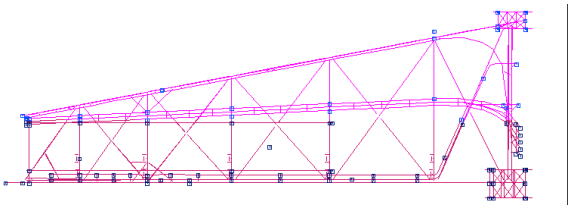

Figure 5.10: Side view of the jacket 18.65m submerged.

The RAO's of the jacket for surge, heave and pitch are given in Figure: 5.11. They are compared with the behaviour of the jacket in air and the behaviour of the jacket 8 meter submerged. It can be seen that the effect on the higher period mode is limited. But the pitch peak at the low period peak is reduced significantly.

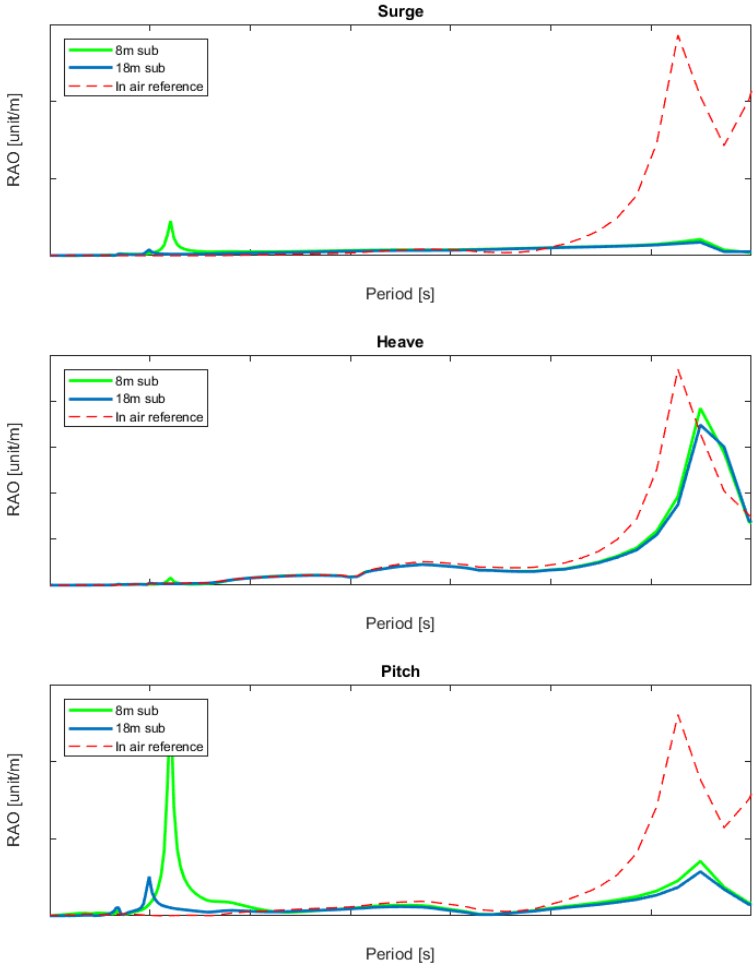

Figure 5.11: The effect of submerged depth on the jacket RAO's.

Tugger winches

Tugger winches are added at the bottom on the crane and are connected to the mainblocks. The goal is to reduce the pitch mode of the jacket. Two tuggerlines per mainblock are applied. This is visualised in Figure: 5.12. A constant damping is set on each of the winches [19]. The result on the pitch RAO is given in Figure: 5.13. It can be seen from the figure that the pitch mode peak is almost completely damped by the tugger winches.

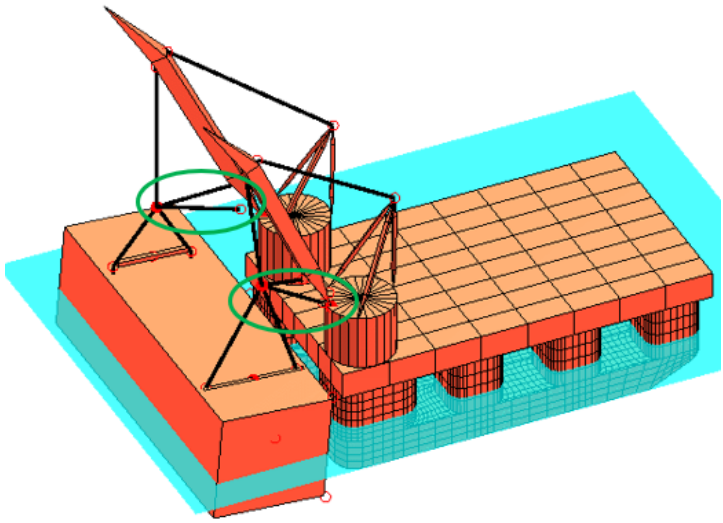

Figure 5.12: Tuggerlines attached to the mainblocks of the Thialf.

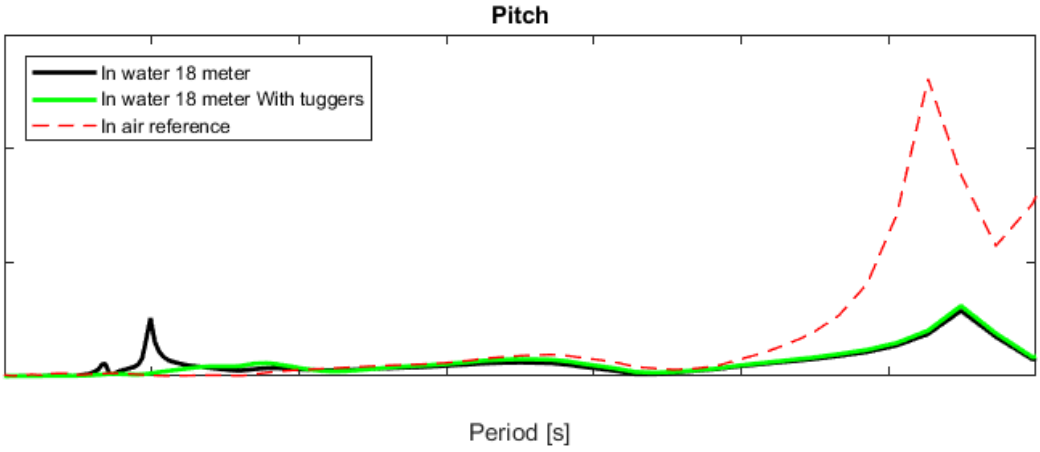

Figure 5.13: The effect of adding tuggerlines on the jacket pitch RAO.

6

Verification

In this section the verification of the submerged jacket model from 5.2, the absolute velocity approach is performed. It is investigated if the formulas are implemented correctly in Moses and the conversion between the different programs is done properly. Comments about the order of magnitude are already made in the explanation of the different influences. But two aspects will be studied in greater detail here namely: the wave surge force on the full jacket and the forces on one leg. Since this is a new method for Heerema there is no measurement data available to validate the model with. But the model of the in air behaviour is compared to measurements. And it proved to be a good starting point. The parts, which are new, are related to the force of the water on the jacket. The formulas which are interned to determine these parts are widely validated. So by verifying the model a first step is made towards validating the whole model. First the wave force will be studied. And secondly the added mass, damping and wave force on one leg are investigated by performing a hand calculation and comparing them to the Moses output.

Concerning the surge wave force on the jacket it is determined where the peaks and trough of the wave force are expected. The force is presented in Figure: 6.1, with the period on the horizontal axis, the amplitude on the primary vertical axis and the phase angle w.r.t. the wave on the secondary axis. The distance between the two submerged legs is about 40 meters. With the use of linear wave theory it can be reasoned and calculated at what periods the peaks and trough are expected in the wave force.

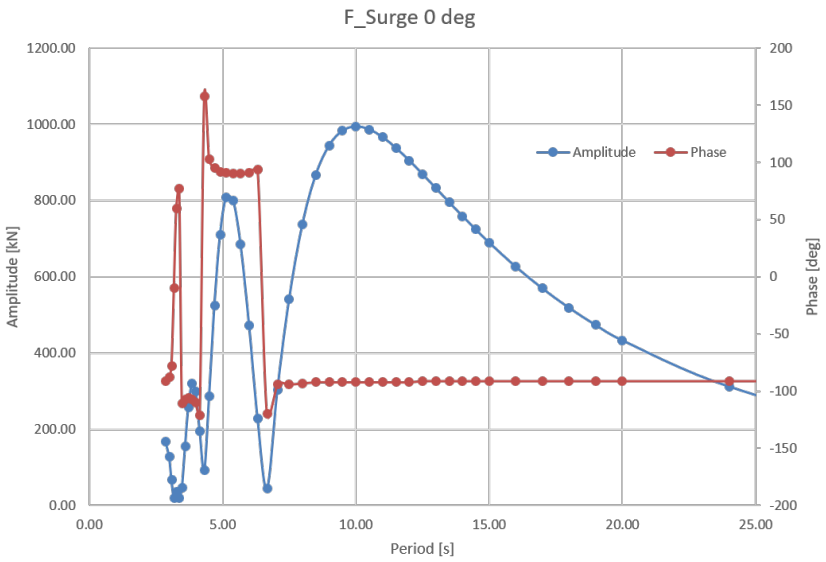

Figure 6.1: Surge wave force in the jacket with waves coming from 0 deg.

A peak in the wave force is expected if the distance between the two legs is exactly the wavelength. In that case the maximum force on each of the legs occurs at the same time. The corresponding period at which this occurs is calculated in Equation: 6.1 and 6.2. A second peak is expected if distance between the legs is 1/4 of the wavelength. From that period and for higher periods the wave force on both legs is acting in the same direction. But the wave acceleration (and velocity) is also decreasing for higher periods. Therefore it is expected that after the peak the wave force decreases almost linearly. The second peak is calculated in Equations: 6.3 and 6.4. The calculated periods match exactly with the wave force peak as calculated by Moses.

$$X_{leg} = \lambda \approx 1.56 \cdot T^2 [m] \tag{6.1}$$

$$T_{peak} = \sqrt{\frac{X_{leg}}{1.56}} = \sqrt{\frac{40}{1.56}} = 5.1 [s] \tag{6.2}$$

$$X_{leg} = \frac{1}{4}\lambda \approx \frac{1}{4} \cdot 1.56 \cdot T^2 [m] \tag{6.3}$$

$$T_{peak_{II}} = \sqrt{\frac{4 \cdot X_{leg}}{1.56}} = 10 [s] \tag{6.4}$$

A trough of the wave force is expected if the distance between the legs is half a wavelength. The wave is then completely out of phase at the two legs. Therefore a minimum in the wave force is expected there. This trough is calculated in Equations: 6.5 and 6.6. The resulting period of 7 seconds is corresponding with the trough as shown in Figure: 6.1.

$$X_{leg} = \frac{1}{2}\lambda \approx \frac{1}{2} \cdot 1.56 \cdot T^2 [m] \tag{6.5}$$

$$T_{trough} = \sqrt{\frac{2 \cdot X_{leg}}{1.56}} = 7 [s] \tag{6.6}$$

6.1. Forces on leg

To verify the forces that Moses calculates the output of Moses for one leg will be compared to hand calculations. The bottom leg of the jacket is modelled separately in SACS and then converted tot Moses in the same way this is done for the entire jacket. The leg consists of three parts, with the largest diameter at the bottom of the leg and the smallest at the top of leg. The leg is 8.65m submerged and the origin is located at bottom of the leg and the axes system is shown in Figure: 6.2. The center of buoyancy is located at $[x, y, z] = [0, 63.93, 0]$ from the origin. The dimensions of the leg are presented in Table 6.1. For the leg the added mass, the damping due to the jacket velocity and the wave force are determined and compared to the output of Moses.

Table 6.1: Dimensions jacket leg.

	D [m]	**L [m]**	**t [m]**	**CoB part to CoB Leg [m]**
Part 1	1.30	46.3	0.08	57.92
Part 2	1.70	16.7	0.08	26.42
Part 3	2.20	82.0	0.08	22.93

Figure 6.2: Bottom leg jacket.

The added mass and the added mass due to the water that is in the flooded leg is determined. For the horizontal and vertical added mass Equation: 6.7 is used per part with Ca=1. And for the resulting added mass moment of inertia Equation: 6.8 is used. The arm to the CoB of the leg is determined for each point on the part and then integrated per part. The total added mass in surge direction for the whole jacket, calculated in Section 5.6, is 3545 [t]. The added mass of two legs is 1414 [t], which means that the two legs account for 40% of the added mass in surge direction.

$$A_{Fpart} = \frac{\pi}{4} \cdot \rho_w \cdot C_a \cdot (D_{out}^2 + D_{in}^2) \cdot L_{part} \tag{6.7}$$

$$A_{Mpart} = \int_{begin-CoB}^{end-CoB} y^2 \cdot A \cdot dy = \frac{1}{3}(y_{begin-CoB}^3 - y_{end-CoB}^3) \cdot \frac{\pi}{4} \cdot \rho_w \cdot C_a \cdot (D_{out}^2 + D_{in}^2) \tag{6.8}$$

Table 6.2: Added mass calculation and comparison to Moses.

Direction	$\mathbf{A}_1$	$\mathbf{A}_2$	$\mathbf{A}_2$	$\mathbf{A}_{total}$ $[t]$ and $[t \cdot m^2]$	$\mathbf{A}_{Moses}$ $[t]$ and $[t \cdot m^2]$	% ***of Moses***
x	111	71	594	**776**	**777**	*1.00*
y	0	0	0	**0**	**0**	*1.00*
z	111	71	594	**776**	**777**	*1.00*
rx	393728	51020	645393	**1090141**	**1090421**	*1.00*
ry	0	0	0	**0**	**0**	*1.00*
rz	393728	51020	645393	**1090141**	**1090421**	*1.00*

The damping due to the jacket velocity is determined next. This is done by calculating the damping force per direction and per part according to the Equations: 6.9 and 6.11. The following velocities are used during this calculation: [x, y, z]= [1, 2, 3] m/s and $[\dot{rx}, \dot{ry}, \dot{rz}]$= [1, 2, 3,] deg/s. The drag coefficient is determined based on smooth members and the Reynolds number per part, as shown in Figure: 6.3. The velocities at each point on the leg are determined based on the the rotational velocity ($\dot{rx}$) and the arm to the CoB of the leg (r). With this velocity and arm the drag coefficient and the resulting moment around the CoB can be determined. The resulting forces and moments due to the (rotational) velocity are presented in Tables: 6.3 and 6.4 respectively.

$$F_{Dpart} = \frac{1}{2} \cdot \rho_w \cdot C_D |\dot{x}| \dot{x} \cdot L_{part} \tag{6.9}$$

$$v_{point} = \omega \cdot r = (\frac{\pi}{180} \cdot \dot{rx}) \cdot r \tag{6.10}$$

$$M_{Dx} = \sum_{y=0}^{y=145} F_{Dz} \cdot r_{point-CoB} \tag{6.11}$$

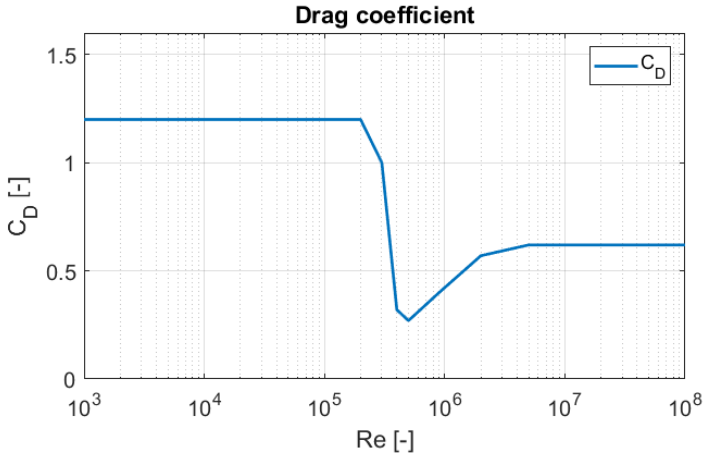

Figure 6.3: Drag coefficient based on Reynolds number[37].

Table 6.3: Damping force calculation and comparison to Moses in kN.

	Part 1			**Part 2**			**Part 3**			**Total**		
	Re	**Cd**	**Drag**	**Re**	**Cd**	**Drag**	**Re**	**Cd**	**Drag**	**F_{Dtot}**	**F_{DMoses}**	**%Moses**
x	1.74E+06	0.50	-15.4	1.74E+06	0.50	-7.27	2.26E+06	0.57	-52.7	**-75.4**	**-75.1**	**1.00**
y	3.49E+06	0.57	0.00	3.49E+06	0.57	0.00	4.51E+06	0.57	0.00	**0.0**	**0.0**	**1.00**
z	5.23E+06	0.62	-158	5.23E+06	0.62	-81.2	6.77E+06	0.62	-515	**-755**	**-764**	**0.99**

Table 6.4: Damping moments, around CoB, calculation compared to Moses.

	Total		
Direction	**M_{Dtot}** [kNm]	**M_{DMoses}** [kNm]	**% Moses**
rx	**-22500**	**-22351**	**1.01**
ry	**0.0**	**0.0**	**1.00**
rz	**-2163**	**-2101**	**1.03**

The wave force is calculated next. It consists of a drag and an inertia depended part. Due to symmetry of the leg the force in surge and heave direction are the same, so only the surge force is explained in this section. Since the leg is horizontally submerged the wave velocity and wave acceleration are constant over the length of the leg, but do vary per wave period. The wave velocity and acceleration are calculated based on Equation: 3.6 and 3.10 for each period and H_s=1m. A constant drag coefficient of 1.2 and inertia coefficient of 2 are used. The wave force and moment per meter wave height are calculated according to Equation: 6.14 and 6.15 and the results are presented in Figure: 6.4.

$$\frac{F_{Dpart}}{\zeta_a} = \frac{1}{2} \cdot \rho_w \cdot D \cdot Cd \cdot u^2 \cdot \frac{L_{part}}{\zeta_a} \tag{6.12}$$

$$\frac{F_{Ipart}}{\zeta_a} = \frac{\pi}{4} \cdot D^2 \cdot \rho_w \cdot Cm \cdot \dot{u} \cdot \frac{L_{part}}{\zeta_a} \tag{6.13}$$

$$F_{wave} = \sqrt{(F_{D1} + F_{D2} + F_{D3})^2 + (F_{I1} + F_{I2} + F_{I3})^2} \tag{6.14}$$

$$M_{wave} = \sqrt{(F_{D1} \cdot r_1 + F_{D2} \cdot r_2 + F_{D3} \cdot r_3)^2 + (F_{I1} \cdot r_1 + F_{I2} \cdot r_2 + F_{I3} \cdot r_3)^2} \tag{6.15}$$

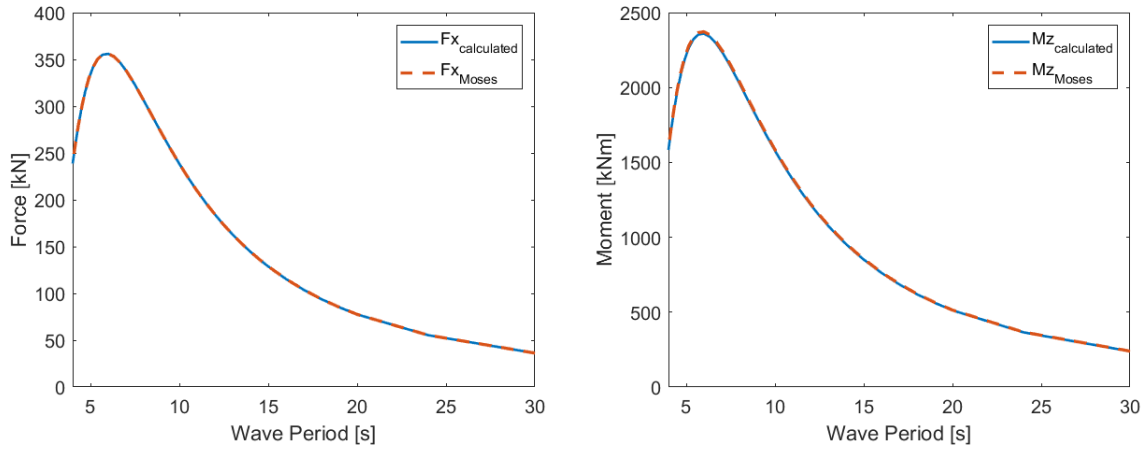

(a) Morison wave force in surge direction.

(b) Morison wave moment around CoB in yaw direction.

Figure 6.4: Wave force and moment comparison.

From all of the above mentioned it is concluded that Moses can be used to accurately determine the forces of the water and the waves on a structure based on the absolute velocity Morison approach. It has been verified that the peaks/trough in the wave force are at the expected periods. And from the calculations on the leg it is shown that Moses can correctly calculate the added mass, including the effect of a flooded member. The Reynolds depended damping force due to the jacket (rotational) velocity matches the hand calculations. And the wave force and moment over a large range of periods correspond with the hand calculation as well.

6.2. Relative velocity approach

As a check the damping force for the different parts in x, y and z are compared to the damping force for the whole jacket. The results are given in the Table 6.5. It can be seen from the table that cutting the jacket into parts does leads to a small change in force if the same velocities are used.

Table 6.5: A comparison of the horizontal and vertical damping forces.

	Left	**Middle**	**Right**	**Total parts**	**Whole jacket**
Fx [kN]	28.12	42.54	29.99	**100.7**	**98.2**
Fy [kN]	0.02	0.12	0.02	**0.2**	**0.2**
Fz [kN]	2.74	6.84	2.87	**12.5**	**12.4**

It was noted from the RAO calculations in Section 5.2.2 that the damping has a large influence on the response of the jacket near the pitch mode at 6s. To determine the applicability of the relative velocity approach the amplitude of the motion is compared to the diameter of the members. According to DNV the approach is valid for r/D>1. The significant single amplitudes of the motion have been derived from the model made in Section 5.2.2 and are presented in Table 5.9 . Where D_{lmax} = 2.2m, D_{lmin} = 1.3m and D_{brace} = 0.4m. It can be seen that for the brace the relative velocity would be valid in heave direction. The approach is also valid for part of the leg and brace.

Table 6.6: Applicability relative velocity approach.

	$\mathbf{x}_a$ [m]	**r/Dlmax**	**r/Dlmin**	**r/Dbrace**
x	0.28	0.1	0.2	0.7
y	0.05	0.0	0.0	0.1
z	0.75	0.3	0.6	**1.9**
rx	0.1	0.0	0.1	0.3
ry	1.8	0.8	**1.4**	**4.5**
rz	0.1	0.0	0.1	0.3

7

Results

In this chapter the operability of the model is determined. The operability of the in air model is compared to the submerged jacket model and the different submerged depths are compared. Lastly the affect of adding tuggerwinches on the operability is presented.

The operability is calculated based on the theory described in Section 3.4. The limits that are used are described in Section 3.4. As an input the different RAO's are used, for in air they are determined with the model from Section 4.1 and for the submerged case the RAO's are determined from the models in Section 5.2. With this RAO's the Significant Double Amplitudes are determined, based on a JONSWAP spectrum with 1m Hs, which are used to the determine the Single Most Probable Maximum for a 3 hour window. With the SMPM and the defined limits the operability is determined for waves coming from 0, 45 and 90 degrees. And they are presented in Figure: 7.3 and 7.4.

The Thialf pitch operability, with the jacket 8.65m submerged and waves from 0 degrees, is determined as example in Figure: 7.1 and Figure: 7.2. With each JONSWAP spectrum and the Thialf pitch RAO the corresponding SDA is determined. The results of which are plotted in Figure: 7. The SMPM is determined and the pitch limit is plotted as well. From Figure: 7.2a it can be seen that the Thialf pitch SMPM cross at a certain period. Therefore it can be seen in Figure: 7 that the operability limit at that period is 1m Hs. And for the lower periods a higher wave height is allowed, since the SMPM is less, and for higher periods the opposite. This operability curve is also shown in the top left plot of Figure: 7.3b.

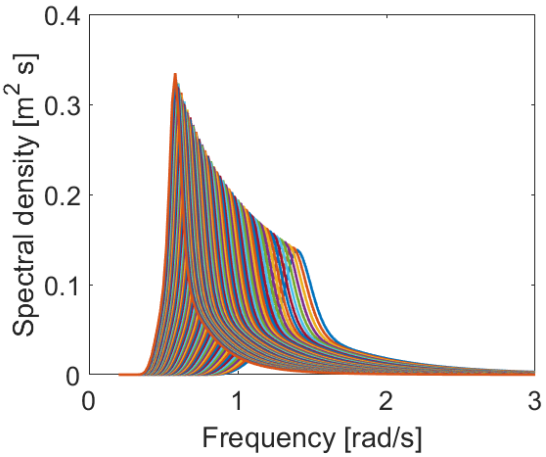

(a) JONSWAP spectra with Hs=1m and Tp=4-20s.

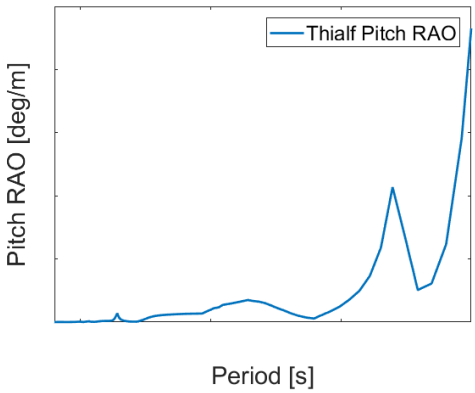

(b) Thialf pitch RAO.

Figure 7.1: JONSWAP specta and Thialf pitch RAO with jacket 8.65m submerged.

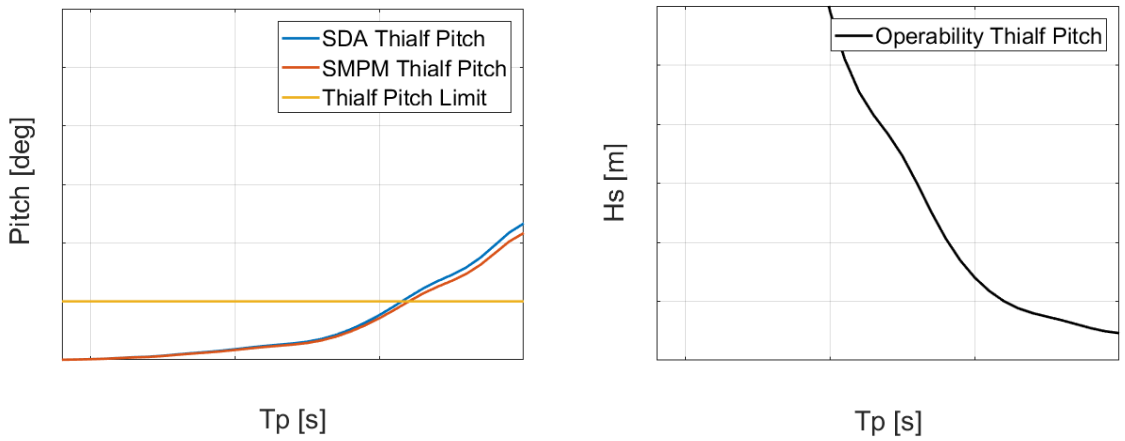

(a) Thialf Pitch SDA, SMPM and the limit.

(b) Operability Thialf pitch.

Figure 7.2: Thialf pitch response and operability with jacket 8.65m submerged.

For the other limits the same procedure has been performed. For the different models the RAO's for Thialf roll and pitch, offlead and sidelead, the dynamic forces in the hoistwires and slings and the clearance between the Thialf and the jacket have been derived. The SMPM has been derived and used to determine the operability based on the limits. The results for 0, 45 and 90 degrees wave direction are given. Each of the grouped criteria are discussed in succession. The grouped criteria are shown per case in Figure: 7.3 and Figure: 7.4. More detailed figures per criteria are included in Appendix D.2.

Jacket in air compared to jacket 8.65m submerged

The operability based on the model with the jacket in air, Figure: 7.3a, is compared here to the operability resulting from the model with the jacket 8.65m submerged, Figure: 7.3b, (bottom legs submerged, Figure: 5.2). First the roll and pitch motions of the Thialf are considered. For both scenarios the pitch is the governing one of the two for waves from 0 degrees. The behaviour is slightly better when the jacket is submerged. For waves from 45 degrees the roll behaviour is mostly the limiting one. Here the motion is marginally improved. And for the waves of 90 degrees is the roll behaviour is slightly worse.

Secondly the offlead and sidelead are considered. Sidelead is defined as relative angle between the crane tip and the load perpendicular to the vessel. And offlead as the angle between the crane tip and the load in line with the vessels surge direction. They are visualised in Figure: 3.9. From the plots of the operability with waves coming from 0 deg and 45 deg it can be seen that if the jacket is in the water the operability is reduced tremendously. This is due to the jacket pitch mode around 6s, that was determined in Section 5.2.2. Due to the pitching of the jacket the slings and hoistwire start slinging back and forth which directly influence the offlead angle. For both directions the operability is reduced to significantly at the natural period. For waves coming from 90 deg the operability due to sidelead improves a little bit.

Thirdly the load fluctuations on the wires are considered. A DAF of 1.3 in air and 1.9 in water is used here. This assures that there will be no slack sling in the wires, which could lead to very high snap loads. The operability is determined based on the dynamic force in the wires and a limit of 0.3 or 0.9 times the static forces in the wires. In air they are not limiting in all directions. Once the jacket is submerged the operability of reduces, even though a higher DAF is used. It can be seen that, especially for waves coming from 0 deg, the slings experience a higher load fluctuation near the jacket pitch mode which leads to a reduced operability. But the DAF limit is not a governing criterion in any of the cases.

Lastly the clearance between the jacket and the Thialf is considered. Fortunately it is not limiting in both cases for all directions. But it should definitely be considered as one of the important, hard limits and thus operability criteria. Since a collision could lead to very serious consequences. When comparing the two cases it can be seen that the clearance improves a lot when the jacket is submerged.

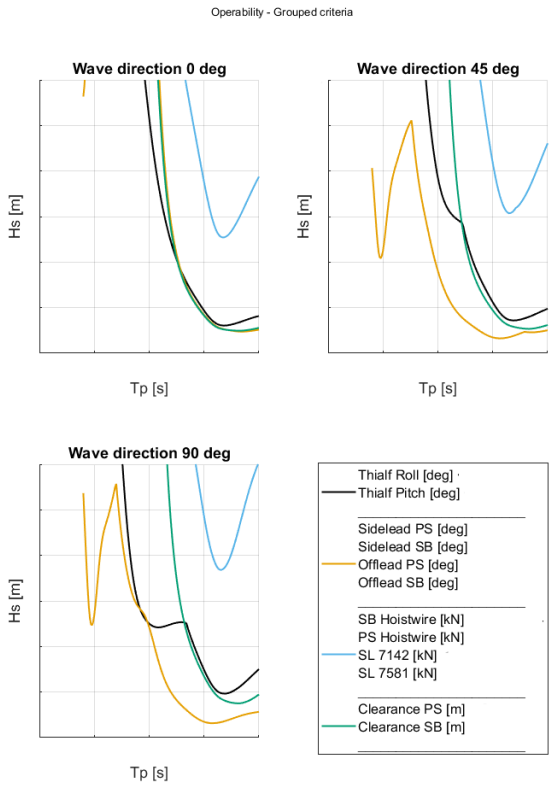

(a) Operability curves with the jacket **in air** for the limiting criteria.

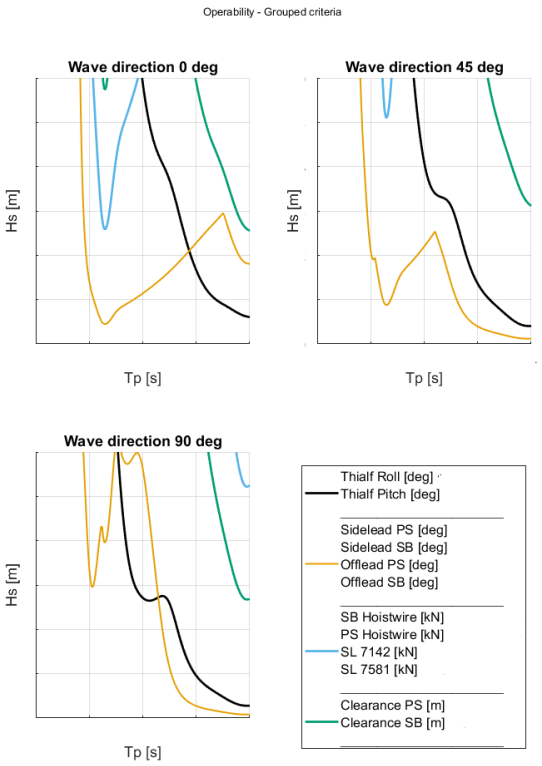

(b) Operability curves with the jacket **8.65 m submerged** for the limiting criteria.

Figure 7.3: Operability curves for jacket in air vs. 8.65m.

Jacket 8.65m submerged compared to jacket 18.65m submerged

The operability of the two models made in Section 5.4 are presented in Figure: 7.4b and 7.5. By submerging the jacket deeper in to the water the operability improves. The jacket gets more resistance to the pitch mode due to the increase in added mass and the reduction on the wave force on the bottom legs (since they are deeper below the wave crest). This results in a higher limit for the offlead peak at the pitch mode. For wave coming from 0 deg the operability for waves with lower periods is still governed by the pitch mode. For the waves with longer periods and the other wave directions the operability improves significantly. The largest improvement is with waves from 45 deg, the operability at the pitch peak period, the allowable wave height more than triples.

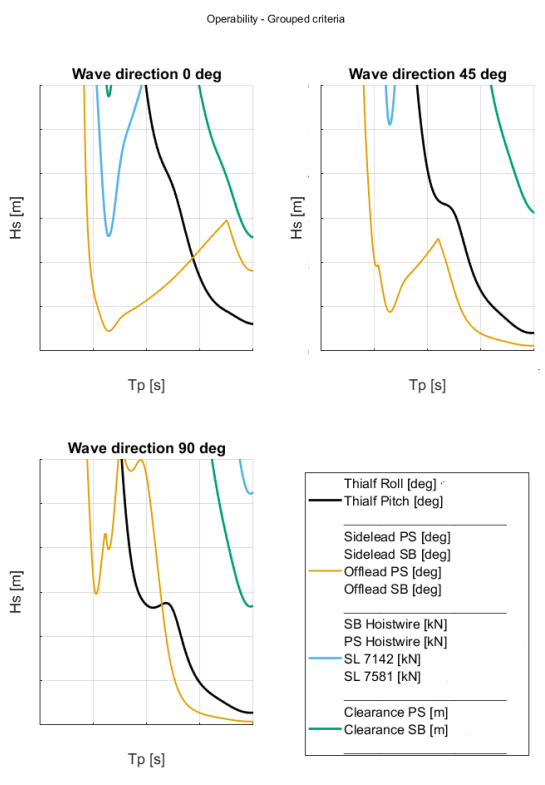

(a) Operability curves with the jacket **8.65 m submerged** for the limiting criteria.

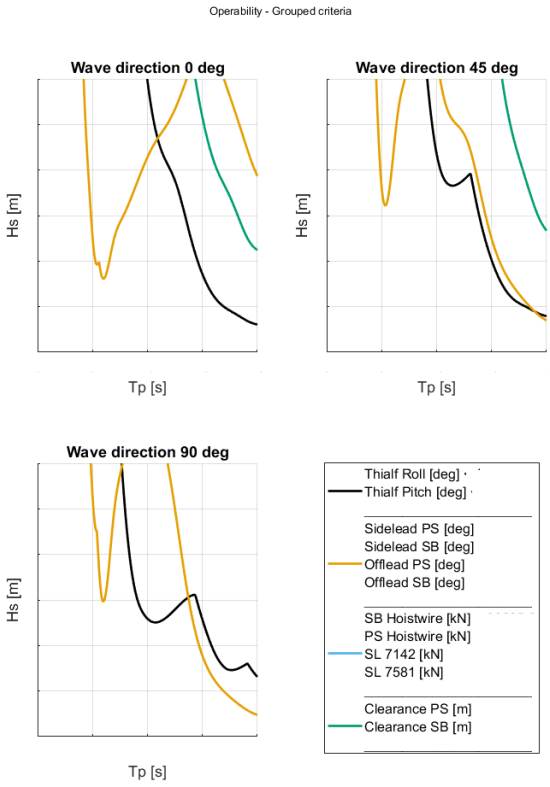

(b) Operability curves with the jacket **18 meters submerged** for the limiting criteria.

Figure 7.4: operability curves for jacket 8.65m vs. 18m submerged.

When adding tuggerlines to the mainblocks the operability can be improved further, as presented in Figure: 7.5. The tuggerlines configuration is shown in Figure: 5.12. As expected they only influence the offlead and sidelead angle near the pitch mode. For the rest the influence on the other limits and higher periods is marginal.

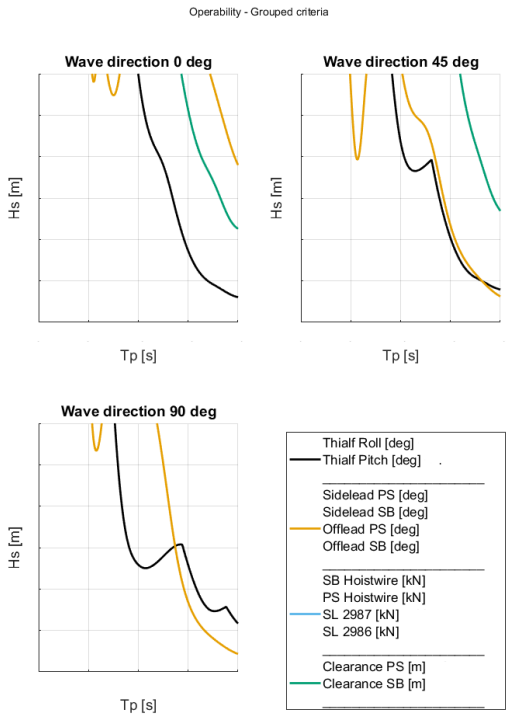

Figure 7.5: Operability curves with the jacket 18 meters submerged with tuggerlines for the limiting criteria.

8

Conclusion & Recommendations

In this chapter the conclusions and recommendations are presented. The 3 sub-question and the main research question are answered first. Thereafter the recommendations are given for improving the research, general considerations and future research.

8.1. Conclusions

The following research questions have been formulated in Chapter 2. They will be answered one by one in this section. First all the sub-questions and after that the main research question. Eventually the additional conclusion are formulated.

1. How does the free hanging jacket in air behave?
    - The jacket behaviour is analysed by comparing the measured response to the model response. It was determined that there are several modes of interest when looking at the RAO's.
    - Although the Thialf's response was low due to the nice weather during the measurements campaign the modes where captured accurately.
2. Which are the relevant forces and how can they and the resulting motions be determined?
    - The relevant forces on the jacket are the wave forces. These forces can be determined by using the Morison equation.
    - The impact of the wind force appeared to be minor when looking at the behaviour of the jacket in water, and it can therefore be neglected.
3. How should one submerge the jacket to reduce the motions as much as practically possible based on a case study of the North Sea jacket?
    - When the jacket is submerged it should be submerged more than a few meters. At first it will mainly attract wave loads. By submerging it deeper the damping and the added mass increases.
    - The relative velocity approach leads to a decrease in damping. This is due to the effect of modelling the jacket in parts.
    - Adding tugger winches to the jacket can improve the behaviour since it can be used to damp out a specific peak, the pitch peak of the jacket in this case.

How does the response of a crane suspended jacket and the vessel change if the jacket is (partly) submerged in water compared to in air?

- When the jacket is submerged in the water it attracts wave loading. This excitation force triggers the low damped pitch mode of the jacket.

- By submerging the jacket only a few meters this lead to a large reduction in operability.
- If the jacket is being submerged deeper it gains additional damping and added mass. This reduces the pitch peak and improves the operability.
- The response to higher periods wave improves when submerging the jacket deeper in the water.
- Submerging the jacket can be used as a contingency scenario for (unexpected) swell waves. But it is crucial to know the behaviour of the jacket. Because submerging it at the wrong depth could lead to large resonant responses. Based on the North Sea jacket case the jacket legs should be outside the wave dominant zone.
- The response with the jacket in the water can be modelled in the frequency domain. But estimating the right damping turned out to be quite difficult. A new approach has been developed.

8.2. Recommendations

This study demonstrates the feasibility of submerging the jacket as a contingency scenario. To explore the other options with a submerged jacket or increase the accuracy of the model recommendations are made in this section.

- Perform more measurements to get more reliable data of the movement of the free hanging jacket. To gain more insight in the behaviour while the jacket is in the water scale model tests can be performed. In that way the Thialf and the full size jacket are not put at risk.
- The jacket velocity values that are used by Heerema may not always be suited for the investigations of the submerged jacket case. It is therefore recommended that an iteration is performed until the jacket velocity converges.
- To improve the relative velocity damping approach, while the jacket is just submerged, a way to accurately determine the forces on parts must be sought. By modelling it in parts the damping increases, although the relative velocity approach gives more damping than the absolute velocity approach. For this study it is more straightforward to submerge the jacket deeper and thereby increase the damping.
- It is recommended to study the affect of submerging a jacket vertically instead of horizontally. Other behaviour of the jacket is expected here. Whether or not this will be positive needs to be determined. If it is positive it could be expanded by investigating the feasibility of wet transport.
- It is recommended to continue this work by expanding the model to include forward speed. That way it can be investigated if sailing with a partly submerged jacket is possible.
- If there is a strong current it could influence the behaviour of the jacket. It is recommended to investigate if this improves or worsens the operation.

Bibliography

[1] P Barclay, C. Schoenmaekers. Dual crane lift systems - sc 211. *Heerema Marine Contractors: Inhouse*, 2016.

[2] J. van den Berg. Frigg qp jacket gets 'on the move' at marin. *MARIN Magazine*, 2009.

[3] J.-C. Berger. The frigg cessation project. *Society of Petroleum Engineers*, 2011.

[4] A.S. Bull and Milton S.L. Worldwide oil and gas platform decommissioning: A review of practices and reefing options. *Ocean Coastal Management*, 168, 2019. URL `http://www.sciencedirect.com/science/article/pii/S0964569118304484`.

[5] S.K. Chakrabarti. *Hydrodynamics of offshore structures*. World Scientific Publishing Co., 1987.

[6] Lehmann E. Östergaard C. Clauss, G. *Offshore Strucutres*. Springer-Verlag London, 1994.

[7] OSPAR commission. Convention for the protection of the marine environment of the north-east atlantic. 1992.

[8] Heerema Marine Contractors. *Liftdyn theory manual*, 2009.

[9] Heerema Marine Contractors. Multimedia gallery, 2020. URL `https://hmc.heerema.com/news-media/multimedia-gallery/`.

[10] J. de Jong. Basis of design for jacket removal, transport & offloading. *Heerema Marine Contractors*, 2000.

[11] O. Faltinsen. *Sea loads on ships and offshore structures*. Cambridge University Press., 1990.

[12] Leo Holthuijsen. Waves in oceanic and coastal waters. *Cambridge University Press:*, 2007.

[13] J. Hoving. Oe44095 bottom founded offshore structures 2019 tu delft, 2019. URL `https://brightspace.tudelft.nl/d2l/le/content/50108/viewContent/711006/View`.

[14] iXblue. Octans. 2019. URL `https://www.ixblue.com/sites/default/files/2020-02/Octans_2019.pdf`.

[15] Mork M. Jenssen, I. Recommended practice for planning, designing and constructing fixed offshore platforms. *NGO Shipbreaking Platform*, 2019.

[16] Massie W.W. Journee, J.M.J. *Offshore Hydromechanics*. Delft University of Technology, 2000.

[17] Connor J.J. Laya, E.J. and S.S. Sunder. Hydrodynamic forceson flexible offshore structures. *J Eng Mech, ASCE, Vol 110*, 1984.

[18] Mathworks. *MATLAB documentation R2020a*, 2020.

[19] G. Meskers and R. Van Dijk. A damping tugger system for offshore heavy lifts. 2012.

[20] Microsoft. *Microsoft Excel Manual*, 2015.

[21] G. Moe and R.L.P. Verley. Hydrodynamic damping of offshore structures in waves and currents. *12th Annual Offshore Technology Conference Houston*, 1980.

[22] J.W. Morison, J.R. Johnson. The force exerted by surface waves on piles. *Journal of Petroleum Technology, 2(05):149–154, 5*, 1950.

[23] P Naaijen. Course notes on motions and loading of structures in waves. *Delft University of Technology*, 2019.

[24] Standards Norway. Norsok n-003: Actions and action effects. 2017.

[25] Basuki R. Nugraha, B. Rigs-to-reef: A new initiative on re-utilization of abandoned offshore oil and gas platforms in indonesia for marine and fisheries sectors. *IOP Conference Series: Earth and Environmental Science*, 241, 2019.

[26] Massachusetts Institute of Technology. *WAMIT Theory Manual*, 1995.

[27] SPT Offshore. Relocation ophir wellhead platform, 2019. URL `https://www.sptoffshore.com/news/malaysia-jitang-field-offshore/`.

[28] Y. Rentoulis. Huldra facilities engineering, preparations and removal. *Heerema Marine Contractors*, 2018.

[29] API RP2A-WSD. Recycling outlook decommissioning of north sea floating oil & gas units. *Houston: American Petroleum Institute*, 2000.

[30] Zoontjes R. Capurso V Samudero, P. Spe-199177-ms-crane suspended transportation – an effective way to remove offshore platforms. *SPE Symposium: Decommissioning and Abandonment*, 2019.

[31] Isaacson M. Sarpkaya, T. *Mechanics of wave forces on offshore structures*. Van Nostrand Reinhold Co New York, 1981.

[32] Shell. Decommissioning in the uk, 2013. URL `https://www.shell.co.uk/sustainability/decommissioning/brent-field-decommissioning/decommissioning-in-the-uk.html`.

[33] A. Slyozkin. Hydrodynamic interaction between floating structures during heavy lift operations - is it worth analysing? *Marine Heavy Transport Lift IV*, 2014.

[34] Saipem S.p.A. Statoil 2/4s removal project, 2014. URL `https://www.gassco.no/globalassets/saipem.pdf`.

[35] Vrouwenvelder A.W.C.M. Klaver E.C. Spijkers, J.M.J. Lecture notes on structural dynamic. *Delft University of Technology*, 2005.

[36] O. Stettner. Floating jacket installation. 2014. URL `http://resolver.tudelft.nl/uuid:c3f0821c-9f1a-460e-bdb5-4a5aac3da95e`.

[37] Bentley Systems. *Reference manual for MOSES*, 2017.

[38] Bentley Systems. *Reference manual for SACS*, 2018.

[39] J. Van Der Tempel, N.F.B. Diepeveen, W.E. De Vries, and D. Cerda Salzmann. Wind energy systems - offshore environmental loads and wind turbine design: impact of wind, wave, currents and ice. 2011.

[40] European Union. Requirements and procedure for inclusion of facilities located in third countries in the european. *Journal of the European Union*, 2016.

[41] Det Norske Veritas. Dnv recommended practice dnv-rp-c205 on environmental conditions and environmental loads. 2006.

[42] Det Norske Veritas. Dnvgl-cg-0130 wave loads - rules and standards. 2018.

[43] W.T. van Wingerden. Floating jacket installation. 2019. URL `http://resolver.tudelft.nl/uuid:dabf39be-c712-48f3-bd44-002f68770dc8`.

Appendices

A

Appendix

A.1. Diffraction theory

The diffraction theory is based on potential theory. It is assumed here that a rigid body is moving in an ideal fluid with harmonic waves. With potential theory the hydrodynamic loads are evaluated. The potential $\Phi(x, y, z, t)$ is based on the superposition of:

- The undisturbed waves potential (Φ_w), this is the wave field as if the vessel is not there.
- The diffraction potential (Φ_d), these are the waves that reflect from the vessel.
- The radiated waves potential (Φ_r), which are the waves that radiate from the vessel due to the motions of the vessel. The waves that radiate are dissipating energy from the ship. This can also be referred to as potential damping.

A brief overview of the theory is given here. For a more elaborate description it is advised to consult Faltinsen [11] or Journee and Massie [16].
It is assumed that the water is incompressible, without viscosity and irrotational. The pressures and velocities can be written in terms of a potential flow. The potential function, Φ, describes the state of the fluid at each point in the water. It has no physical meaning, it is a mathematical expression that can be used to calculate the velocities at a certain point (x, y, z) at time t. The velocity can be obtained by taking the spatial derivative of the potential function and is given in Equation: A.1.

$$\mathbf{V} = \nabla\Phi = \frac{\partial\Phi}{\partial x}\mathbf{i} + \frac{\partial\Phi}{\partial y}\mathbf{j} + \frac{\partial\Phi}{\partial z}\mathbf{k} = u\mathbf{i} + v\mathbf{j} + w\mathbf{k} \tag{A.1}$$

Within the fluid domain the potential function has to fulfil several requirements.

1. **Continuity condition or Laplace Equation**
   With the incompressible flow assumption the velocity potential derived in Equation: A.1 has to satisfy the Laplace equation, as expressed in Equation: A.2.

$$\nabla\mathbf{V} = \nabla^2\Phi = 0 \tag{A.2}$$

2. **Seabed boundary condition**
   This condition allows no fluid to pass through the sea floor. The sea floor is impermeable, therefor the following condition has to be satisfied:

$$\frac{\partial\Phi}{\partial z} = 0 \text{ at the sea floor } z = -h \tag{A.3}$$

3. **Boundary condition at the surface**
   For the free surface dynamic boundary condition the pressure at the free surface of the fluid ($z = 0$) is equal to the atmospheric pressure.

$$\frac{\partial\Phi}{\partial t} + g\zeta = 0 \text{ at } z = 0 \tag{A.4}$$

And the kinematic boundary condition states that at the free surface the vertical motion of the flow has to be identical to the vertical velocity of the free surface itself. This assures that no particles can escape trough the surface. With linearised free surface flow conditions this is given in Equation: A.5:

$$\frac{\partial \Phi}{\partial z} = \frac{\partial \zeta}{\partial t} \text{ at } z = 0 \tag{A.5}$$

A differentiation of Equation: A.4 with respect to t and combined with the kinematic free surface boundary condition gives:

$$\frac{\partial^2 \Phi}{\partial t^2} + g\frac{\partial \Phi}{\partial z} = 0 \text{ at } z = 0 \tag{A.6}$$

4. **Kinematic Boundary Condition on the Oscillating Body Surface**
No fluid can go through the surface of a body. Therefor the velocity normal to the vessel hull is set to the same value as the velocity of the hull in this direction. This boundary condition is also referred to as the "no-leak" condition and is given by:

$$\frac{\partial \Phi}{\partial \eta} = v_\eta x, y, z, t \tag{A.7}$$

5. **Radiation condition** The radiation condition states that the outgoing free surface wave decays appropriately.

$$\lim_{R \to \infty} \Phi = 0 \tag{A.8}$$

The complex potential Φ can be written as a superposition of the undisturbed wave potential Φ_0, the wave diffraction potential Φ_7 and the potentials which describe the body motions in all six directions.

$$\Phi = -i\omega \left[(\Phi_0 + \Phi_7)\zeta_0 + \sum_{j=1}^{6} \Phi_j \zeta_j \right] \tag{A.9}$$

From the linearised Bernoulli equation the pressure of the fluid can be calculated:

$$p(x, y, z, t) = -\rho \frac{\partial \Phi}{\partial t} \tag{A.10}$$

The forces and moments follow from integration of the pressure p, over the submerged surface of the vessel S.

$$\vec{F} = -\int_S \int (p \cdot \vec{n}) dS \tag{A.11}$$

$$\vec{M} = -\int_S \int (p \cdot (\vec{r} \times \vec{n}) dS \tag{A.12}$$

B

Appendix

B.1. Software tools for dynamic analysis

Different software tools are used in this study. Apart from the supposedly known Matlab [18] and Excel [20] more specialised software will be used. The different tools are summarised below.

LIFTDYN (Heerema Marine Contractors [8]). Liftdyn is a in-house computer tool that is designed to model and solve general linear hydrodynamic problems in the frequency domain. Liftdyn can solve systems consisting of rigid bodies connected to each other or to the earth by springs, dampers and hinges. The body may have a frequency depended mass and damping, and frequency depended exciting forces resulting in a frequency depended response or RAO (response amplitude operator) of the system. The mass matrix M is defined by a vessels mass and radii of gyration. The hydrodynamic database for the vessel or the load can be inserted for each body. In case of the SSCV, a standard spring matrix which represents the stiffness of the DP system is added to the spring matrix. The resulting RAO can be post-processed to a motion, velocity or acceleration RAO at any desired point relative to any other point. A RAO of the force in a connector can also be generated. A generated RAO can be used to produce the significant response in a specific sea state. Furthermore, limiting criteria can be defined to obtain operability curves indicating the maximum allowable wave height as a function of the spectral period.

MOSES (Bentley Systems[37]). MOSES is a program that can be used for the hydrostatic and hydrodynamic analysis of offshore platforms and vessels. It can be used to design, simulate and analyse complex offshore structures and installation projects. It is a frequency domain program that can computed the Morison equation and diffraction theory.

WAMIT (Massachusetts Institute of Technology [26]). WAMIT is a program that can be used to analyse wave interactions with offshore structures and vessels. It is a frequency domain program that uses potential wave theory to calculate the inertial forces such as radiation and diffraction. It is based on linear and second order potential theory. It uses a panel method with a certain mesh of the panels to solve the velocity potential on the submerged surfaces of the bodies.

SACS (Bentley Systems [38]). SACS is an integrated finite element structural analysis program. It is widely used by structural engineers. It can be used to design and analyse offshore structures, perform fatigue analysis, design check, grillage & sea fastening designs and structural integrity (e.g.ship impact analysis). Within the scope of the thesis SACS will only be used to get the detailed geometric model of the jacket.

C

Appendix

C.1. Freebody diagram

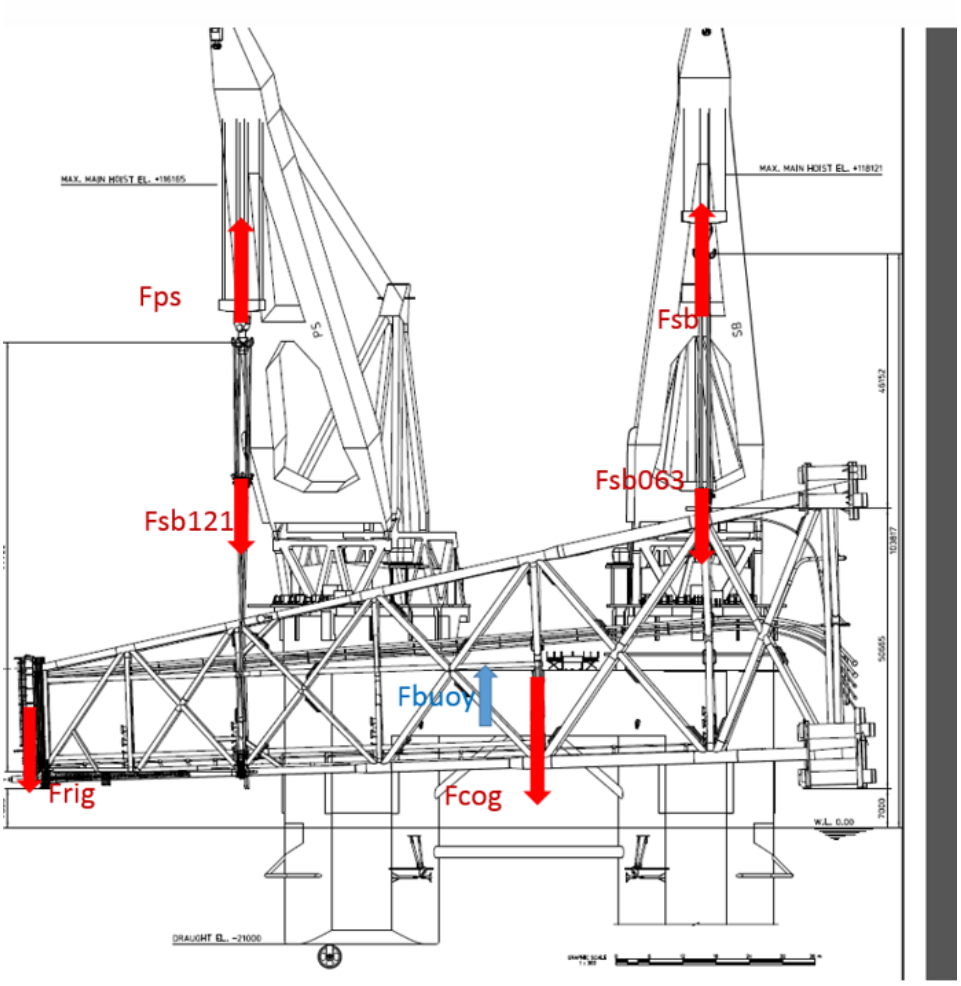

Figure C.1: Free body diagram jacket. Note that Fbuoy is 0 in this case.

D

Appendix

D.1. RAO's absolute velocity approach

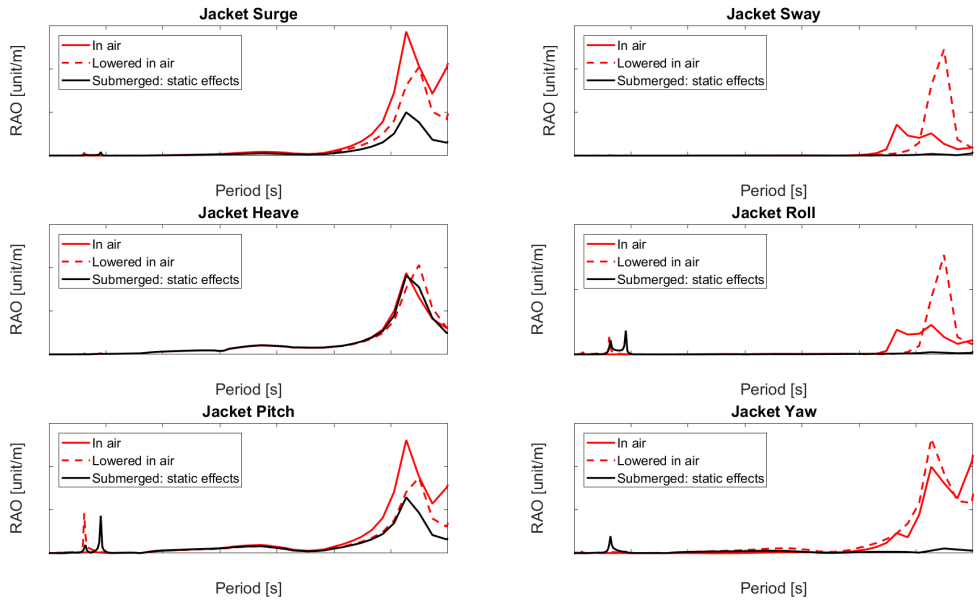

Figure D.1: Jacket RAO's static influences

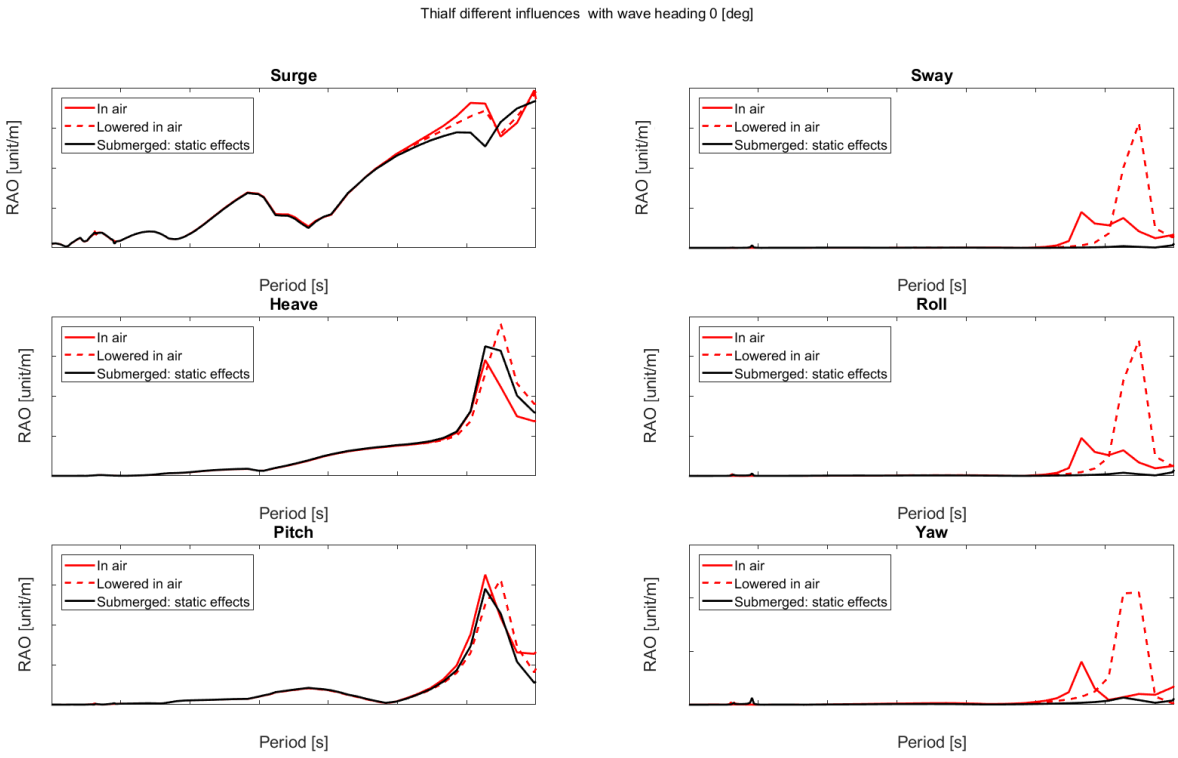

Figure D.2: Thialf RAO's static influences

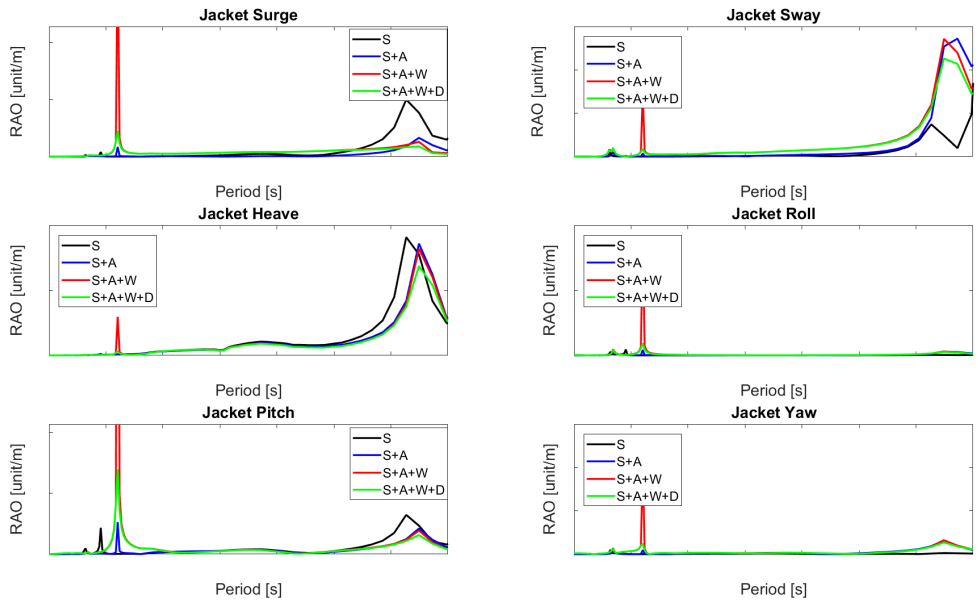

Figure D.3: Jacket RAO's dynamic influences

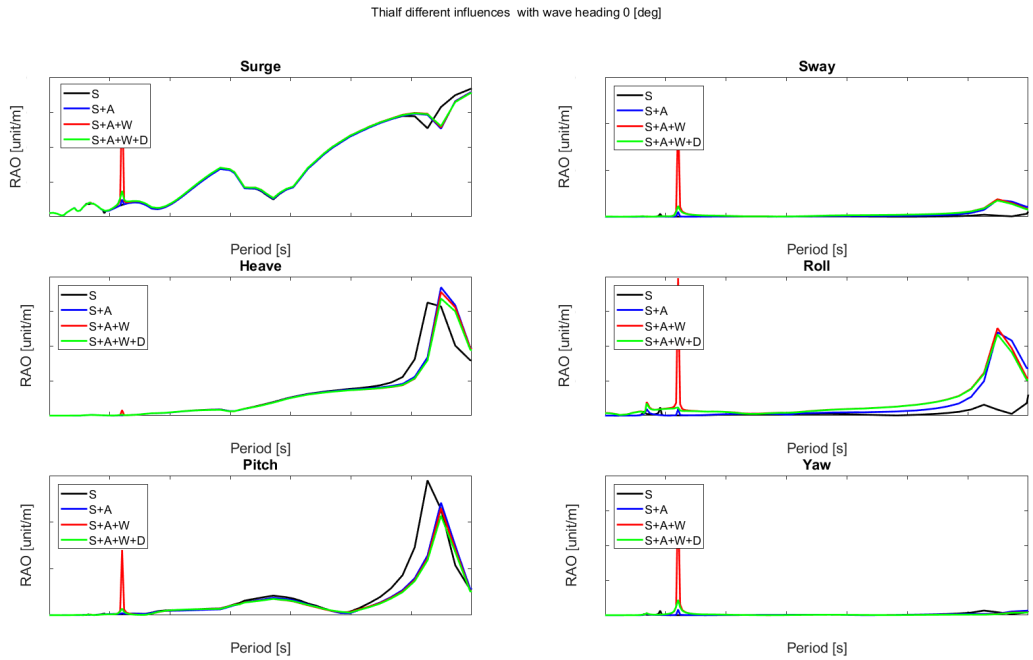

Figure D.4: Thialf RAO's dynamic influences

D.2. Wave force on jacket

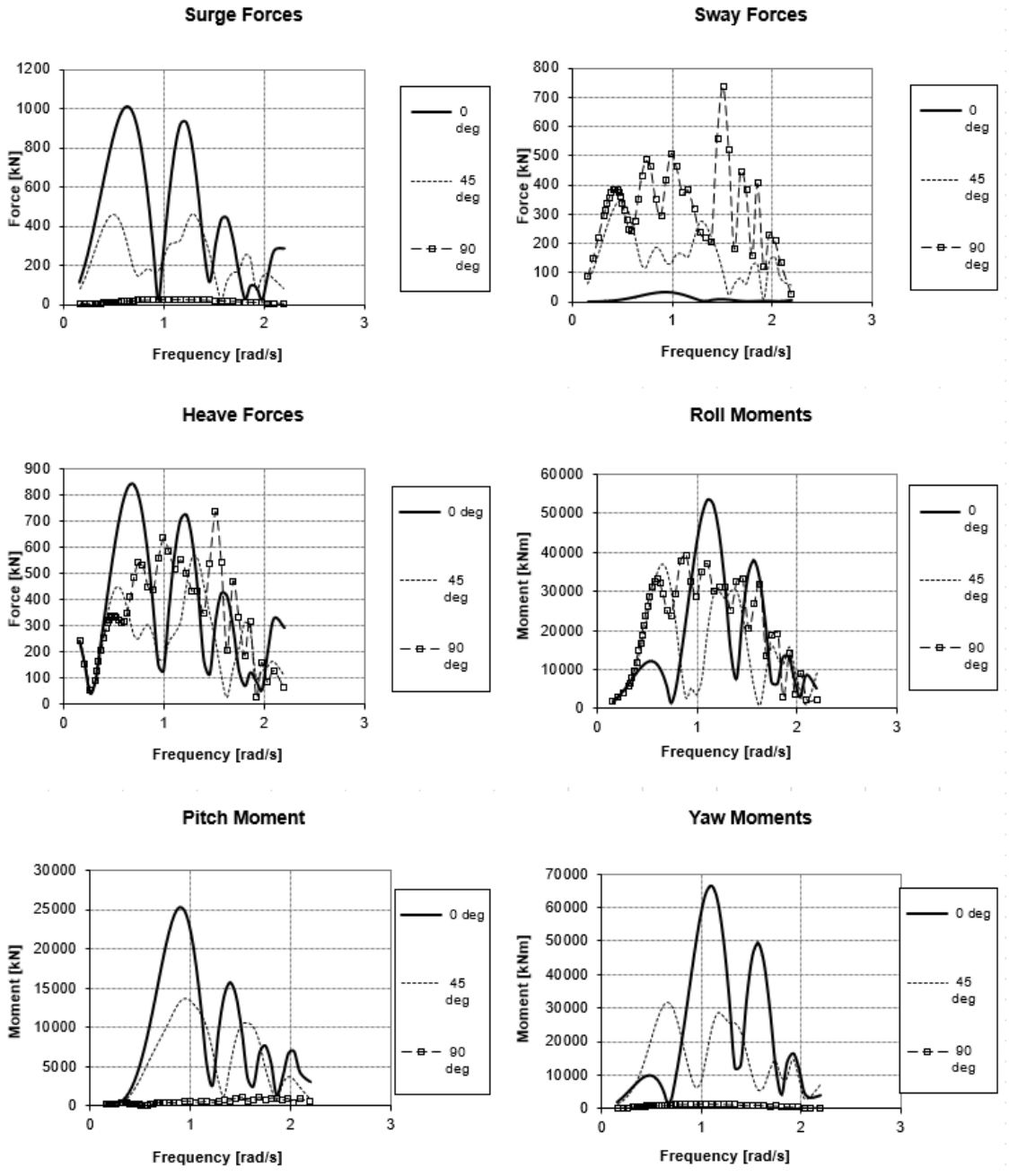

Figure D.5: Wave force on jacket per meter wave height.